

# Solving SU(3) Yang-Mills theory on the lattice: a calculation of selected gauge observables with gradient flow

---

Hans Mathias Mamen Vege

June 23, 2019

Supervisor: *Andrea Shindler*

Co-supervisor: *Morten Hjorth-Jensen*

University of Oslo

## Introduction

---

# Structure

- Quantum Chromodynamics(QCD).

- **QCD.** We will go through and explain what QCD as well as motivate its existence.

# Structure

- Quantum Chromodynamics(QCD).
- Lattice QCD.

1

- **QCD.** We will go through and explain what QCD as well as motivate its existence.
- **LQCD.** We will briefly show how one discretise the lattice and perform calculations on it.

# Structure

- Quantum Chromodynamics(QCD).
- Lattice QCD.
- Gradient flow.

1

- **QCD.** We will go through and explain what QCD as well as motivate its existence.
- **LQCD.** We will briefly show how one discretise the lattice and perform calculations on it.
- **Gradient flow.** We will quickly introduce gradient flow and explain its effects.

# Structure

- Quantum Chromodynamics(QCD).
- Lattice QCD.
- Gradient flow.
- Developing a code for solving  $SU(3)$  Yang-Mills theory.

1

- **QCD.** We will go through and explain what QCD as well as motivate its existence.
- **LQCD.** We will briefly show how one discretise the lattice and perform calculations on it.
- **Gradient flow.** We will quickly introduce gradient flow and explain its effects.
- **GLAC.** Will briefly present the code which we developed as well as some benchmarks. We will also present the Metropolis algorithm.

# Structure

- Quantum Chromodynamics(QCD).
- Lattice QCD.
- Gradient flow.
- Developing a code for solving  $SU(3)$  Yang-Mills theory.
- Results.

1

- **QCD.** We will go through and explain what QCD as well as motivate its existence.
- **LQCD.** We will briefly show how one discretise the lattice and perform calculations on it.
- **Gradient flow.** We will quickly introduce gradient flow and explain its effects.
- **GLAC.** Will briefly present the code which we developed as well as some benchmarks. We will also present the Metropolis algorithm.
- **Results.** We will present the results obtained from pure gauge calculations.

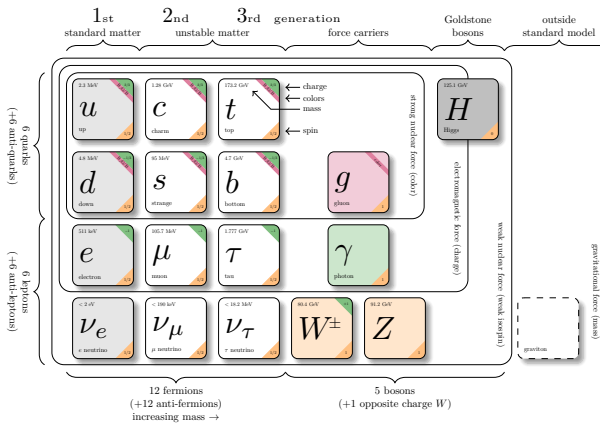
# Structure

- Quantum Chromodynamics(QCD).
- Lattice QCD.
- Gradient flow.
- Developing a code for solving  $SU(3)$  Yang-Mills theory.
- Results.

## Quantum Chromodynamics(QCD)

---

# The Standard Model



Consists of the innermost square of the **six quarks** and the **eight gluons**.

# The non-linearity of QCD

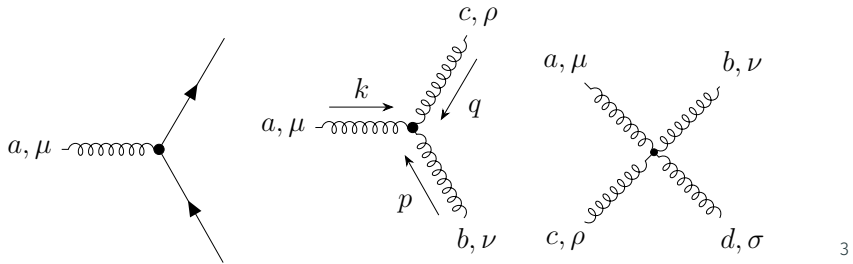
The QCD Lagrangian

$$\mathcal{L}_{\text{QCD}} = \sum_{f=1}^{N_f} \bar{\psi}^{(f)} \left( i \not{D} - m^{(f)} \right) \psi^{(f)} - \frac{1}{4} G_{\mu\nu}^a G^{a\mu\nu},$$

with action

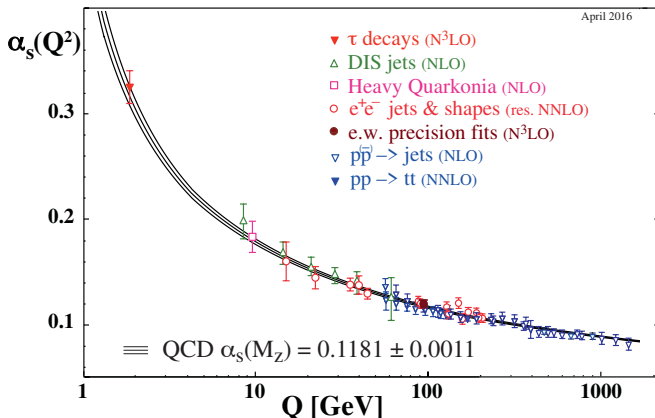
$$S = \int d^4x \mathcal{L}_{\text{QCD}}, \quad (1)$$

is invariant under a SU(3) symmetry.



- *Gluon self-interaction.*
- This central aspect is mostly covered in the pure-gauge/Yang-Mills section of the theory.
- **Two important features:** *confinement* and *asymptotic freedom*.

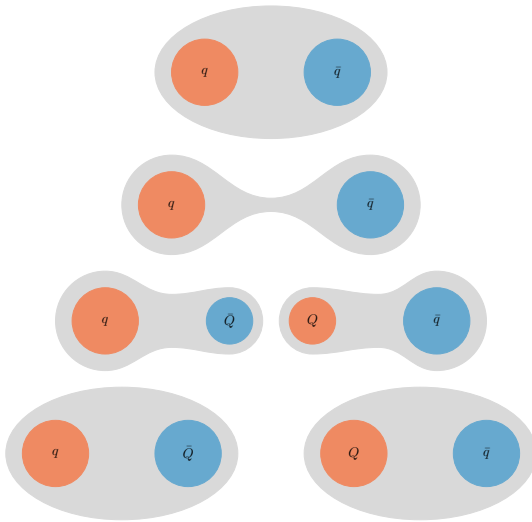
# Asymptotic freedom



4

- The coupling constant **decreases** as we **increase** the energy.
- Also serves as an *experimental proof* of QCD.
- Other lines of *evidence*: triple  $\gamma$  decay and muon cross section ratio  $R$ .
  - Triple  $\gamma$  decay: the number of colors is included in the cross section, which can be measured experimentally.
  - Muon cross section ratio  $R$ : the ratio is dependent on having three colors.

# Confinement



5

If we try to pull apart **two quarks in a meson**, more and more energy is required until we have enough energy to spontaneously create a **quark-antiquark pair**, forming thus **two new mesons**.

# Lattice Quantum Chromodynamics(LQCD)

---

# Discretizing spacetime

1. Divide spacetime into a cube of size  $N^3 \times N_T$ .

Make a quick drawing perhaps of a lattice?

## Discretizing spacetime

1. Divide spacetime into a cube of size  $N^3 \times N_T$ .
2. Fermions live on the each *point* in the cube.

Make a quick drawing perhaps of a lattice?

## Discretizing spacetime

1. Divide spacetime into a cube of size  $N^3 \times N_T$ .
2. Fermions live on the each *point* in the cube.
3. The gauge fields live on the sites *in between* the points, and is called links.

Make a quick drawing perhaps of a lattice?

# Discretizing spacetime

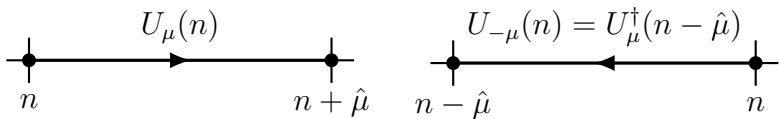
1. Divide spacetime into a cube of size  $N^3 \times N_T$ .
2. Fermions live on the each *point* in the cube.
3. The gauge fields live on the sites *in between* the points, and is called links.

Goal: *maintain gauge invariance*.

Make a quick drawing perhaps of a lattice?

## Links

A link connects one lattice site to another and is a  $SU(3)$  matrix.



where  $U_{-\mu}(n) = U_\mu(n - \hat{\mu})^\dagger$ .

- Defined from the gauge transporter.
- A link in the positive  $\hat{\mu}$  direction is shown in the figure to the left.
- A link in the negative  $\hat{\mu}$  direction is shown in the figure to the right.

## Gauge invariance on the lattice

Links constructed such that we maintain gauge invariance in the action,

## Gauge invariance on the lattice

Links constructed such that we maintain gauge invariance in the action,

$$U_\mu(n) \rightarrow U'_\mu(n) = \Omega(n) U_\mu(n) \Omega(n + \hat{\mu})^\dagger,$$
$$U_{-\mu}(n) \rightarrow U'_{-\mu}(n) = \Omega(n) U_\mu(n - \hat{\mu})^\dagger \Omega(n - \hat{\mu})^\dagger.$$

## Gauge invariance on the lattice

Links constructed such that we maintain gauge invariance in the action,

$$U_\mu(n) \rightarrow U'_\mu(n) = \Omega(n) U_\mu(n) \Omega(n + \hat{\mu})^\dagger,$$
$$U_{-\mu}(n) \rightarrow U'_{-\mu}(n) = \Omega(n) U_\mu(n - \hat{\mu})^\dagger \Omega(n - \hat{\mu})^\dagger.$$

Two main types of gauge invariant objects,

## Gauge invariance on the lattice

Links constructed such that we maintain gauge invariance in the action,

$$U_\mu(n) \rightarrow U'_\mu(n) = \Omega(n) U_\mu(n) \Omega(n + \hat{\mu})^\dagger,$$
$$U_{-\mu}(n) \rightarrow U'_{-\mu}(n) = \Omega(n) U_\mu(n - \hat{\mu})^\dagger \Omega(n - \hat{\mu})^\dagger.$$

Two main types of gauge invariant objects,

- Objects with fermions  $\psi, \bar{\psi}$  as end points.

## Gauge invariance on the lattice

Links constructed such that we maintain gauge invariance in the action,

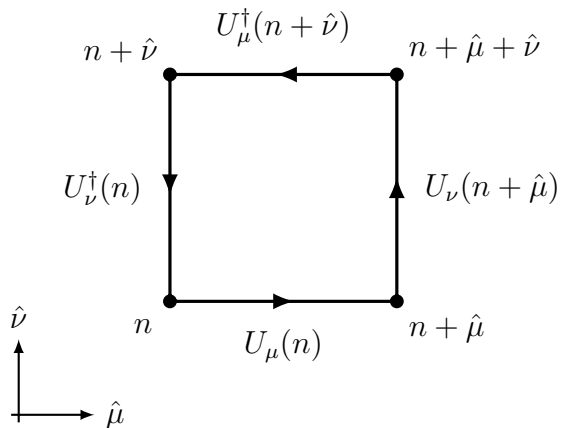
$$U_\mu(n) \rightarrow U'_\mu(n) = \Omega(n) U_\mu(n) \Omega(n + \hat{\mu})^\dagger,$$
$$U_{-\mu}(n) \rightarrow U'_{-\mu}(n) = \Omega(n) U_\mu(n - \hat{\mu})^\dagger \Omega(n - \hat{\mu})^\dagger.$$

Two main types of gauge invariant objects,

- Objects with fermions  $\psi, \bar{\psi}$  as end points.
- Fully connected gauge invariant objects(i.e. “loops”).

# The plaquette

The simplest gauge invariant object,



## The Wilson gauge action

The Wilson gauge action is given as

$$S_G[U] = \frac{\beta}{3} \sum_{n \in \Lambda} \sum_{\mu < \nu} \text{Re} \operatorname{tr} [1 - P_{\mu\nu}(n)], \quad (2)$$

with  $\beta = 6/g_S^2$ .

Continuum action recovered when  $a \rightarrow 0$ !

- Using the definition of the link we saw earlier, we can reproduce the continuum action up to a discretization error of  $\mathcal{O}(a^2)$ .

# Developing a code for solving SU(3) Yang-Mills theory on the lattice

---

A lattice configuration consists of  $3 \times 3$  SU(3) matrices,

- The SU(3) matrices are  $3 \times 3$  matrices of nine complex numbers or 18 real numbers.
- This leads to an absolute **requirement of efficiency**, both in **calculations** and in **input/output**.
- When returning to what ensembles of configurations we generated this will be evident.

# The numerical challenge in lattice QCD

A lattice configuration consists of  $3 \times 3$  SU(3) matrices,

$$\underbrace{N^3}_{\text{Spatial}} \times \underbrace{N_T}_{\text{Temporal}} \times \underbrace{4}_{\text{Links}} \times \underbrace{9}_{\text{SU(3) matrix}} \times \underbrace{2}_{\mathbb{C}\text{-numbers}} = 72N^3N_T,$$

- The SU(3) matrices are  $3 \times 3$  matrices of nine complex numbers or 18 real numbers.
- This leads to an absolute **requirement of efficiency**, both in **calculations** and in **input/output**.
- When returning to what ensembles of configurations we generated this will be evident.

# The numerical challenge in lattice QCD

A lattice configuration consists of  $3 \times 3$  SU(3) matrices,

$$\underbrace{N^3}_{\text{Spatial}} \times \underbrace{N_T}_{\text{Temporal}} \times \underbrace{4}_{\text{Links}} \times \underbrace{9}_{\text{SU(3) matrix}} \times \underbrace{2}_{\mathbb{C}\text{-numbers}} = 72N^3N_T,$$

$\rightarrow 8 \times 72N^3N_T$  bytes.

- The SU(3) matrices are  $3 \times 3$  matrices of nine complex numbers or 18 real numbers.
- This leads to an absolute **requirement of efficiency**, both in **calculations** and in **input/output**.
- When returning to what ensembles of configurations we generated this will be evident.

# The path integral

$$\langle O \rangle = \frac{1}{Z} \int \mathcal{D}U O[\psi, \bar{\psi}, U] e^{-S_G[U] - S_F[\psi, \bar{\psi}, U]}.$$

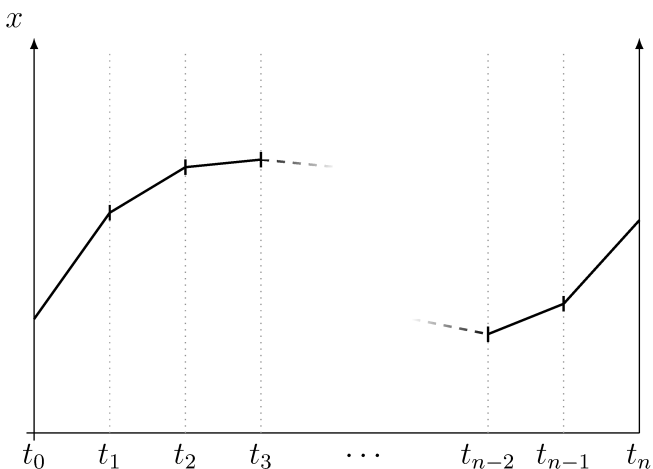
$$Z = \int \mathcal{D}U \mathcal{D}\bar{\psi} \mathcal{D}\psi e^{-S_G[U] - S_F[\psi, \bar{\psi}, U]}.$$

# The path integral

$$\langle O \rangle = \frac{1}{Z} \int \mathcal{D}U O[U] e^{-S_G[U]}.$$

$$Z = \int \mathcal{D}U e^{-S_G[U]}.$$

# The path integral



- An example of the discretized path integral, going from time  $t_0$  to  $t_n$ , where the end points is taken to be equal,  $x_0 = x_{N_T}$ . We integrate over all of space at each time  $t_i$  finding the most likely position at a given time.

# The path integral

$$\langle O \rangle = \frac{1}{Z} \int \mathcal{D}U O[U] e^{-S_G[U]}.$$

with

$$Z = \int \mathcal{D}U e^{-S_G[U]}.$$

- An example of the discretized path integral, going from time  $t_0$  to  $t_n$ , where the end points is taken to be equal,  $x_0 = x_{N_T}$ . We integrate over all of space at each time  $t_i$  finding the most likely position at a given time.
- We will use the parts marked in red as a probability distribution which we will create configurations from.

# The path integral

$$\langle O \rangle = \frac{1}{Z} \int \mathcal{D}U O[U] e^{-S_G[U]}.$$

with

$$Z = \int \mathcal{D}U e^{-S_G[U]}.$$

We will use the *Metropolis algorithm* to create configurations of the lattice.

- An example of the discretized path integral, going from time  $t_0$  to  $t_n$ , where the end points is taken to be equal,  $x_0 = x_{N_T}$ . We integrate over all of space at each time  $t_i$  finding the most likely position at a given time.
- We will use the parts marked in red as a probability distribution which we will create configurations from.
- This can be used in the *Metropolis algorithm*.

# The path integral

$$\langle O \rangle = \frac{1}{Z} \int \mathcal{D}U O[U] e^{-S_G[U]}.$$

with

$$Z = \int \mathcal{D}U e^{-S_G[U]}.$$

We will use the *Metropolis algorithm* to create configurations of the lattice.

- An example of the discretized path integral, going from time  $t_0$  to  $t_n$ , where the end points is taken to be equal,  $x_0 = x_{N_T}$ . We integrate over all of space at each time  $t_i$  finding the most likely position at a given time.
- We will use the parts marked in red as a probability distribution which we will create configurations from.
- This can be used in the *Metropolis algorithm*.
- Since a path integral integrates over all possible configurations, our job us to generate enough configurations to properly represent the statistics.

# The path integral

$$\langle O \rangle = \frac{1}{Z} \int \mathcal{D}U O[U] e^{-S_G[U]}.$$

with

$$Z = \int \mathcal{D}U e^{-S_G[U]}.$$

We will use the *Metropolis algorithm* to create configurations of the lattice.

- An example of the discretized path integral, going from time  $t_0$  to  $t_n$ , where the end points is taken to be equal,  $x_0 = x_{N_T}$ . We integrate over all of space at each time  $t_i$  finding the most likely position at a given time.
- We will use the parts marked in red as a probability distribution which we will create configurations from.
- This can be used in the *Metropolis algorithm*.
- Since a path integral integrates over all possible configurations, our job us to generate enough configurations to properly represent the statistics.

## Measurements on the lattice

The observable becomes an average over the  $N_{\text{MC}}$  gauge configurations.

$$\langle O \rangle = \lim_{N_{\text{MC}} \rightarrow \infty} \frac{1}{N_{\text{MC}}} \sum_i^{N_{\text{MC}}} O[U_i]$$

We now need to generate configurations...

- We perform an average of the created configurations.

## Parallelization

The lattice now is a 4D hypercube, with four links associated to each lattice site → need to parallelize!

- Due to the size of the lattice, we need to parallelize!.

# Parallelization

The lattice now is a 4D hypercube, with four links associated to each lattice site → need to parallelize!

Two methods used:

- Due to the size of the lattice, we need to parallelize!.
- We parallelized using **MPI**.

# Parallelization

The lattice now is a 4D hypercube, with four links associated to each lattice site → need to parallelize!

Two methods used:

- Single link sharing used in the Metropolis algorithm.

15

- Due to the size of the lattice, we need to parallelize!.
- We parallelized using **MPI**.
- Tested out **halos**, but turned out to be problematic when generating.

# Parallelization

The lattice now is a 4D hypercube, with four links associated to each lattice site → need to parallelize!

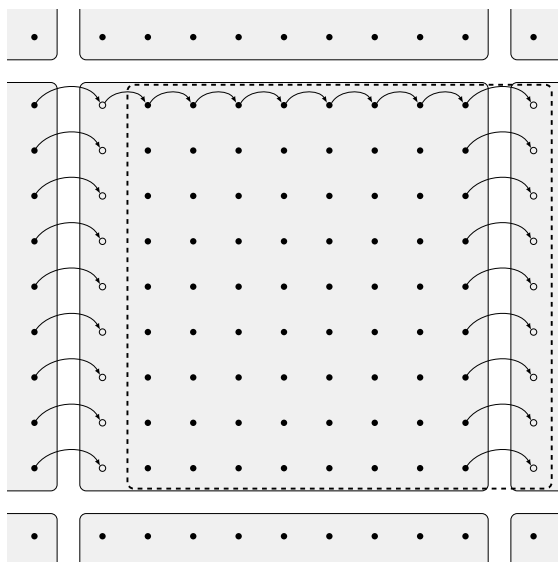
Two methods used:

- Single link sharing used in the Metropolis algorithm.
- *shifts* used in gradient flow and observable sampling

15

- Due to the size of the lattice, we need to parallelize!.
- We parallelized using **MPI**.
- Tested out **halos**, but turned out to be problematic when generating.

# Shifts



16

- An illustration of the lattice shift.
- The links  $U_\nu$  of the lattice are copied over to a temporary lattice shifted in direction  $\hat{\mu}$ .
- The face that is shifted over to an adjacent sub-lattice is shared through a non-blocking MPI call, while we copy the links to the temporary lattice.
- Allows for a simplified syntax close to that of the equations we are working with.
- Don't have to write out any loops over the lattice positions.

## Gradient flow

---

## The flow equation

The flow of the SU(3) gauge fields are denoted by  $B_\mu(x, t_f)$  which are Lie algebra valued gauge fields,

$$\frac{d}{dt_f} B_\mu(x, t_f) = D_\nu G_{\nu \mu}(x, t_f), \quad (3)$$

- The flow equation in the continuum is defined by this differential equation.

## The flow equation

The flow of the SU(3) gauge fields are denoted by  $B_\mu(x, t_f)$  which are Lie algebra valued gauge fields,

$$\frac{d}{dt_f} B_\mu(x, t_f) = D_\nu G_{\nu \mu}(x, t_f), \quad (3)$$

$$D_\mu = \partial_\mu + [B_\mu(x, t_f), \cdot], \quad (4)$$

- The flow equation in the continuum is defined by this differential equation.
- With the covariant derivative given by following, with the  $\cdot$  being the derivative with respect to flow time.

## The flow equation

The flow of the SU(3) gauge fields are denoted by  $B_\mu(x, t_f)$  which are Lie algebra valued gauge fields,

$$\frac{d}{dt_f} B_\mu(x, t_f) = D_\nu G_{\nu \mu}(x, t_f), \quad (3)$$

$$D_\mu = \partial_\mu + [B_\mu(x, t_f), \cdot], \quad (4)$$

$$G_{\mu\nu}(x, t_f) = \partial_\mu B_\nu(x, t_f) - \partial_\nu B_\mu(x, t_f) - i[B_\mu(x, t_f), B_\nu(x, t_f)], \quad (5)$$

- The flow equation in the continuum is defined by this differential equation.
- With the covariant derivative given by following, with the  $\cdot$  being the derivative with respect to flow time.
- The field strength tensor of the flown fields is given in the regular format.

## The flow equation

The flow of the SU(3) gauge fields are denoted by  $B_\mu(x, t_f)$  which are Lie algebra valued gauge fields,

$$\frac{d}{dt_f} B_\mu(x, t_f) = D_\nu G_{\nu \mu}(x, t_f), \quad (3)$$

$$D_\mu = \partial_\mu + [B_\mu(x, t_f), \cdot], \quad (4)$$

$$G_{\mu\nu}(x, t_f) = \partial_\mu B_\nu(x, t_f) - \partial_\nu B_\mu(x, t_f) - i[B_\mu(x, t_f), B_\nu(x, t_f)], \quad (5)$$

with the initial conditions being the fundamental gauge field,

$$B_\mu(x, t_f)|_{t_f=0} = A_\mu(x).$$

- The flow equation in the continuum is defined by this differential equation.
- With the covariant derivative given by following, with the  $\cdot$  being the derivative with respect to flow time.
- The field strength tensor of the flown fields is given in the regular format.
- The initial condition is the un-flowed gauge field,  $A_\mu$ .

# The flow equation

The flow of the SU(3) gauge fields are denoted by  $B_\mu(x, t_f)$  which are Lie algebra valued gauge fields,

$$\frac{d}{dt_f} B_\mu(x, t_f) = D_\nu G_{\nu \mu}(x, t_f), \quad (3)$$

$$D_\mu = \partial_\mu + [B_\mu(x, t_f), \cdot], \quad (4)$$

$$G_{\mu\nu}(x, t_f) = \partial_\mu B_\nu(x, t_f) - \partial_\nu B_\mu(x, t_f) - i[B_\mu(x, t_f), B_\nu(x, t_f)], \quad (5)$$

with the initial conditions being the fundamental gauge field,

$$B_\mu(x, t_f)|_{t_f=0} = A_\mu(x).$$

A bad approximation: *the diffusion equation*,

$$\frac{\partial}{\partial t_f} B_\mu(x, t_f) \approx \partial^2 B_\mu(x, t_f)$$

17

- The flow equation in the continuum is defined by this differential equation.
- With the covariant derivative given by following, with the  $\cdot$  being the derivative with respect to flow time.
- The field strength tensor of the flown fields is given in the regular format.
- The initial condition is the un-flowed gauge field,  $A_\mu$ .
- Bad approx.: diffusion equation.

# The flow equation

The flow of the SU(3) gauge fields are denoted by  $B_\mu(x, t_f)$  which are Lie algebra valued gauge fields,

$$\frac{d}{dt_f} B_\mu(x, t_f) = D_\nu G_{\nu \mu}(x, t_f), \quad (3)$$

$$D_\mu = \partial_\mu + [B_\mu(x, t_f), \cdot], \quad (4)$$

$$G_{\mu\nu}(x, t_f) = \partial_\mu B_\nu(x, t_f) - \partial_\nu B_\mu(x, t_f) - i[B_\mu(x, t_f), B_\nu(x, t_f)], \quad (5)$$

with the initial conditions being the fundamental gauge field,

$$B_\mu(x, t_f)|_{t_f=0} = A_\mu(x).$$

A bad approximation: *the diffusion equation*,

$$\frac{\partial}{\partial t_f} B_\mu(x, t_f) \approx \partial^2 B_\mu(x, t_f)$$

The smearing radius increases as  $\sqrt{8t_f}$ .

- The flow equation in the continuum is defined by this differential equation.
- With the covariant derivative given by following, with the  $\cdot$  being the derivative with respect to flow time.
- The field strength tensor of the flown fields is given in the regular format.
- The initial condition is the un-flowed gauge field,  $A_\mu$ .
- Bad approx.: diffusion equation.
- Topological charge preserved and is more pronounced.
- Renormalizes the topological charge at non-zero flow time.

# The flow equation

The flow of the SU(3) gauge fields are denoted by  $B_\mu(x, t_f)$  which are Lie algebra valued gauge fields,

$$\frac{d}{dt_f} B_\mu(x, t_f) = D_\nu G_{\nu \mu}(x, t_f), \quad (3)$$

$$D_\mu = \partial_\mu + [B_\mu(x, t_f), \cdot], \quad (4)$$

$$G_{\mu\nu}(x, t_f) = \partial_\mu B_\nu(x, t_f) - \partial_\nu B_\mu(x, t_f) - i[B_\mu(x, t_f), B_\nu(x, t_f)], \quad (5)$$

with the initial conditions being the fundamental gauge field,

$$B_\mu(x, t_f)|_{t_f=0} = A_\mu(x).$$

A bad approximation: *the diffusion equation*,

$$\frac{\partial}{\partial t_f} B_\mu(x, t_f) \approx \partial^2 B_\mu(x, t_f)$$

The smearing radius increases as  $\sqrt{8t_f}$ .

- The flow equation in the continuum is defined by this differential equation.
- With the covariant derivative given by following, with the  $\cdot$  being the derivative with respect to flow time.
- The field strength tensor of the flown fields is given in the regular format.
- The initial condition is the un-flowed gauge field,  $A_\mu$ .
- Bad approx.: diffusion equation.
- Topological charge preserved and is more pronounced.
- Renormalizes the topological charge at non-zero flow time.

Lattice definition given by

$$\dot{V}_{tf}(x, \mu) = -g_S^2 \left\{ \partial_{x,\mu} S_G[V_{tf}] \right\} V_{tf}(x, \mu),$$

- On the lattice, the flow equation takes the shape in terms of the link variables.

# Gradient flow on the lattice

Lattice definition given by

$$\dot{V}_{tf}(x, \mu) = -g_S^2 \left\{ \partial_{x,\mu} S_G[V_{tf}] \right\} V_{tf}(x, \mu),$$

with initial condition,

$$V_{tf}(x, \mu)|_{t_f=0} = U(x, \mu)$$

- On the lattice, the flow equation takes the shape in terms of the link variables.
- Initial conditions similar to the continuum case.

## Gradient flow on the lattice

Lattice definition given by

$$\dot{V}_{tf}(x, \mu) = -g_S^2 \left\{ \partial_{x,\mu} S_G[V_{tf}] \right\} V_{tf}(x, \mu),$$

with initial condition,

$$V_{tf}(x, \mu)|_{t_f=0} = U(x, \mu)$$

Note: need to find the action derivative  $S_G[V_{tf}]$ .

- On the lattice, the flow equation takes the shape in terms of the link variables.
- Initial conditions similar to the continuum case.
- The action derivative is also needed, but that is a minor task we will not cover here.

## Gradient flow on the lattice

Lattice definition given by

$$\dot{V}_{tf}(x, \mu) = -g_S^2 \left\{ \partial_{x,\mu} S_G[V_{tf}] \right\} V_{tf}(x, \mu),$$

with initial condition,

$$V_{tf}(x, \mu)|_{t_f=0} = U(x, \mu)$$

Note: need to find the action derivative  $S_G[V_{tf}]$ .

- On the lattice, the flow equation takes the shape in terms of the link variables.
- Initial conditions similar to the continuum case.
- The action derivative is also needed, but that is a minor task we will not cover here.

# Solving gradient flow with Runge-Kutta 3

With

$$\dot{V}_{tf} = -g_S^2 \left\{ \partial_{x,\mu} S_G[V_{tf}] \right\} V_{tf} = Z(V_{tf}) V_{tf},$$

- We rewrite the equations slightly,

# Solving gradient flow with Runge-Kutta 3

With

$$\dot{V}_{tf} = -g_S^2 \left\{ \partial_{x,\mu} S_G[V_{tf}] \right\} V_{tf} = Z(V_{tf}) V_{tf},$$

and  $Z_i = \epsilon_f Z(W_i)$  we get

$$W_0 = V_{tf},$$

$$W_1 = \exp \left[ \frac{1}{4} Z_0 \right] W_0,$$

$$W_2 = \exp \left[ \frac{8}{9} Z_1 - \frac{17}{36} Z_0 \right] W_1,$$

$$V_{tf+\epsilon_f} = \exp \left[ \frac{3}{4} Z_2 - \frac{8}{9} Z_1 + \frac{17}{36} Z_0 \right] W_2,$$

with coefficients from Lüscher [3].

- We rewrite the equations slightly,
- and use a structure preserving integrator with coefficients from Lüscher [3].

# Solving gradient flow with Runge-Kutta 3

With

$$\dot{V}_{tf} = -g_S^2 \left\{ \partial_{x,\mu} S_G[V_{tf}] \right\} V_{tf} = Z(V_{tf}) V_{tf},$$

and  $Z_i = \epsilon_f Z(W_i)$  we get

$$W_0 = V_{tf},$$

$$W_1 = \exp \left[ \frac{1}{4} Z_0 \right] W_0,$$

$$W_2 = \exp \left[ \frac{8}{9} Z_1 - \frac{17}{36} Z_0 \right] W_1,$$

$$V_{tf+\epsilon_f} = \exp \left[ \frac{3}{4} Z_2 - \frac{8}{9} Z_1 + \frac{17}{36} Z_0 \right] W_2,$$

with coefficients from Lüscher [3].

- We rewrite the equations slightly,
- and use a structure preserving integrator with coefficients from Lüscher [3].
- We control the accuracy of this integrator by  $\epsilon_f$ .

# Solving gradient flow with Runge-Kutta 3

With

$$\dot{V}_{tf} = -g_S^2 \left\{ \partial_{x,\mu} S_G[V_{tf}] \right\} V_{tf} = Z(V_{tf}) V_{tf},$$

and  $Z_i = \epsilon_f Z(W_i)$  we get

$$W_0 = V_{tf},$$

$$W_1 = \exp \left[ \frac{1}{4} Z_0 \right] W_0,$$

$$W_2 = \exp \left[ \frac{8}{9} Z_1 - \frac{17}{36} Z_0 \right] W_1,$$

$$V_{tf+\epsilon_f} = \exp \left[ \frac{3}{4} Z_2 - \frac{8}{9} Z_1 + \frac{17}{36} Z_0 \right] W_2,$$

with coefficients from Lüscher [3].

- We rewrite the equations slightly,
- and use a structure preserving integrator with coefficients from Lüscher [3].
- We control the accuracy of this integrator by  $\epsilon_f$ .

## Verifying the integration

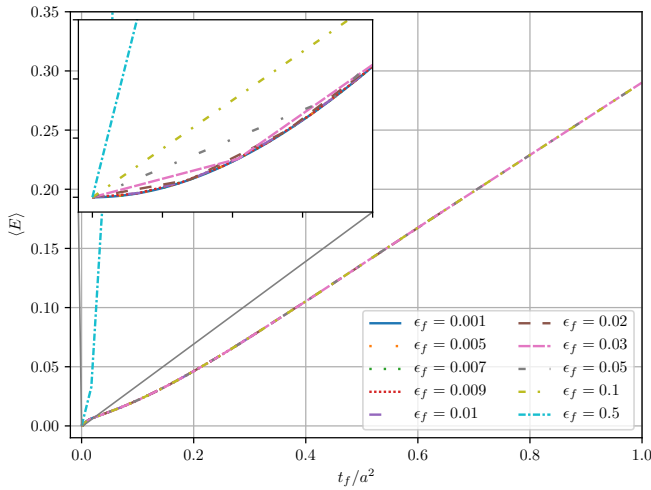
Testing the integrator for different integration steps  $\epsilon_f$ .

$\epsilon_f$	0.001	0.005	0.007	0.009	0.01	0.02	0.03	0.05	0.1	0.5
--------------	-------	-------	-------	-------	------	------	------	------	-----	-----

- The values we will test the integrator against.

## Verifying the integration

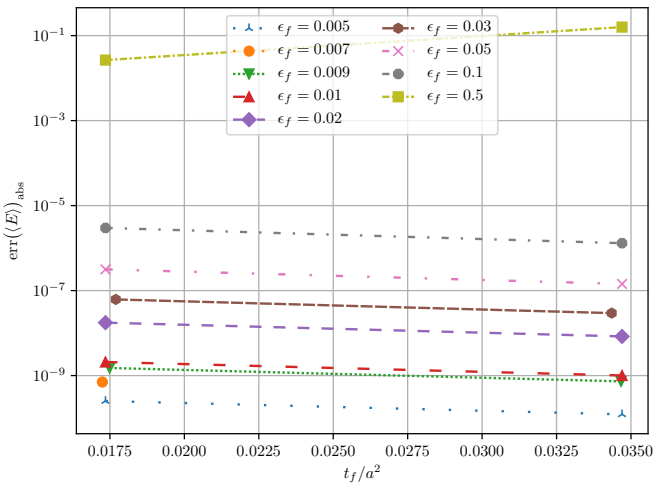
Lattice size  $N^3 \times N_T = 24^3 \times 48$  with  $\beta = 6.0$ .



- The values we will test the integrator against.
- The energy flowed for different the different  $\epsilon_f$  values.

## Verifying the integration

The absolute difference between the smallest flow time  $\epsilon_f = 0.001$  and those shown previously.

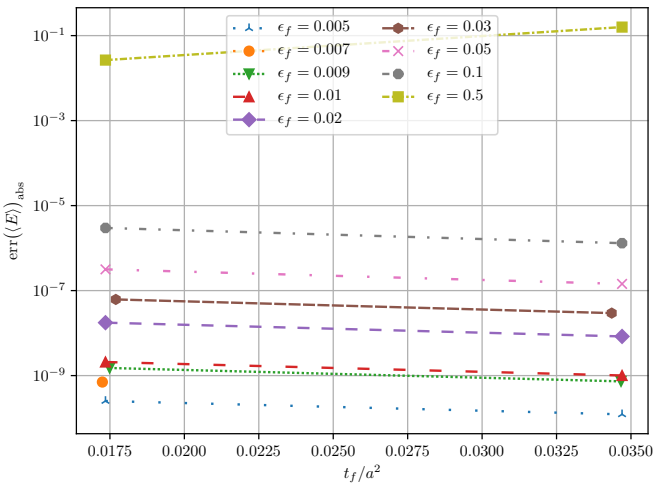


20

- The values we will test the integrator against.
- The energy flowed for different the different  $\epsilon_f$  values.
- The absolute difference between the smallest flow time  $\epsilon_f = 0.001$  and those listed in previous table.
- The reason for **only having two points** is due to the fact that we are **only comparing points** that are **close to each other in flow time**. If we were to have more points, we would have to double the number of flow time steps for the smallest lattices.

## Verifying the integration

The absolute difference between the smallest flow time  $\epsilon_f = 0.001$  and those shown previously.

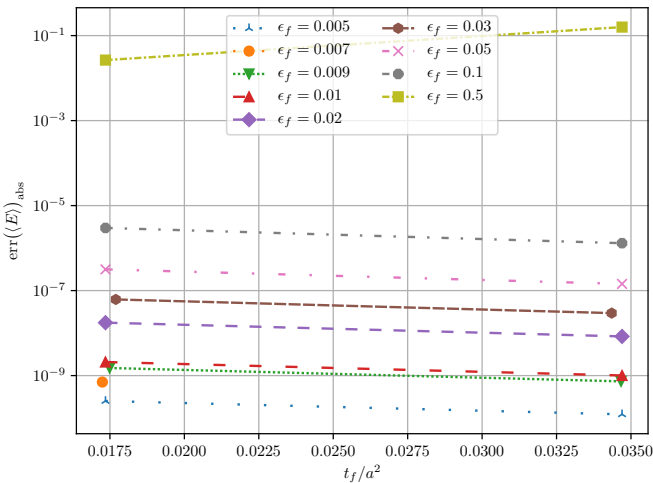


20

- The values we will test the integrator against.
- The energy flowed for different the different  $\epsilon_f$  values.
- The absolute difference between the smallest flow time  $\epsilon_f = 0.001$  and those listed in previous table.
- The reason for **only having two points** is due to the fact that we are **only comparing points** that are **close to each other in flow time**. If we were to have more points, we would have to double the number of flow time steps for the smallest lattices.
- An **example** of the flowing, can be seen by observing the **energy evolving over flow time**.

## Verifying the integration

The absolute difference between the smallest flow time  $\epsilon_f = 0.001$  and those shown previously.



20

- The values we will test the integrator against.
- The energy flowed for different the different  $\epsilon_f$  values.
- The absolute difference between the smallest flow time  $\epsilon_f = 0.001$  and those listed in previous table.
- The reason for **only having two points** is due to the fact that we are **only comparing points** that are **close to each other in flow time**. If we were to have more points, we would have to double the number of flow time steps for the smallest lattices.
- An **example** of the flowing, can be seen by observing the **energy evolving over flow time**.

## Results

---

# Ensembles

Ensemble	$\beta$	$N$	$N_T$	$N_{\text{cfg}}$	$\epsilon_{\text{flow}}$	Config. size[GB]
$A$	6.0	24	48	1000	0.01	0.356
$B$	6.1	28	56	1000	0.01	0.659
$C$	6.2	32	64	2000	0.01	1.125
$D_1$	6.45	32	32	1000	0.02	0.563
$D_2$	6.45	48	96	250	0.02	5.695

- We use  $N_{\text{corr}} = 1600$  for  $\beta = 6.45$  ensembles,  $N_{\text{corr}} = 600$  for the rest.

- The main ensembles made for this thesis.
- Every configuration was flown with  $N_{\text{flow}} = 1000$  flow steps.
- We should also mention that we generated a few additional ensembles for investigating other aspects of the topological charge.

# Ensembles

Ensemble	$\beta$	$N$	$N_T$	$N_{\text{cfg}}$	$\epsilon_{\text{flow}}$	Config. size[GB]
$A$	6.0	24	48	1000	0.01	0.356
$B$	6.1	28	56	1000	0.01	0.659
$C$	6.2	32	64	2000	0.01	1.125
$D_1$	6.45	32	32	1000	0.02	0.563
$D_2$	6.45	48	96	250	0.02	5.695

- We use  $N_{\text{corr}} = 1600$  for  $\beta = 6.45$  ensembles,  $N_{\text{corr}} = 600$  for the rest.
- $N_{\text{up}} = 30$ .

- The main ensembles made for this thesis.
- Every configuration was flown with  $N_{\text{flow}} = 1000$  flow steps.
- We should also mention that we generated a few additional ensembles for investigating other aspects of the topological charge.

## Lattice sizes

Ensemble	$L/a$	$L$ [fm]	$a$ [fm]
$A$	24	2.235(9)	0.0931(4)
$B$	28	2.214(10)	0.0791(3)
$C$	32	2.17(1)	0.0679(3)
$D_1$	32	1.530(9)	0.0478(3)
$D_2$	48	2.29(1)	0.0478(3)

Charge radius of a proton:  $\sim 0.85$  fm.

The lattice sizes.

## Energy definition

$$E = \frac{a^4}{2|\Lambda|} \sum_{n \in \Lambda} \sum_{\mu, \nu} (F_{\mu\nu}^{\text{clov}}(n))^2$$

23

- Defined as the field strength tensor squared averaged over all lattice points and directions.
- We can use this definition to set a scale.

## Energy definition

$$E = \frac{a^4}{2|\Lambda|} \sum_{n \in \Lambda} \sum_{\mu, \nu} (F_{\mu\nu}^{\text{clov}}(n))^2$$

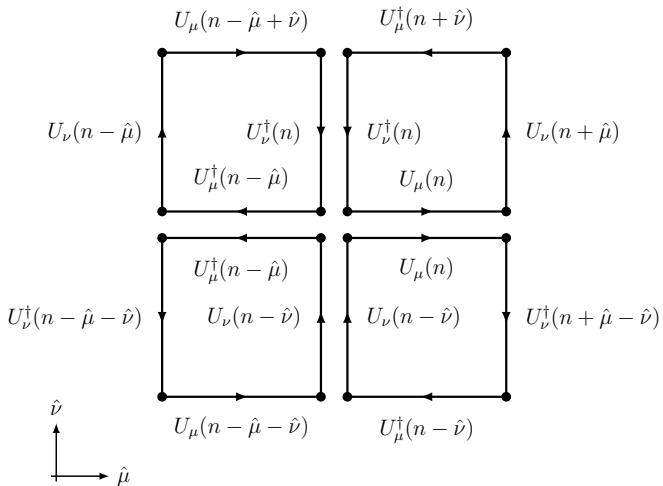
We can use this definition to set a scale  $t_0$ ,

$$\left\{ t_f^2 \langle E(t) \rangle \right\}_{t_f=t_0} = 0.3.$$

- Defined as the field strength tensor squared averaged over all lattice points and directions.
- We can use this definition to set a scale.

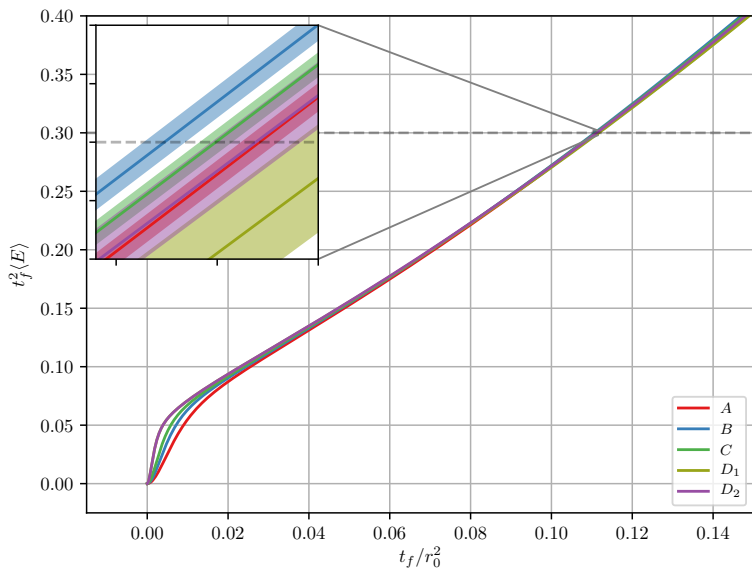
# The clover field strength definition

$F_{\mu\nu}^{\text{clov}}(n)$  is given by

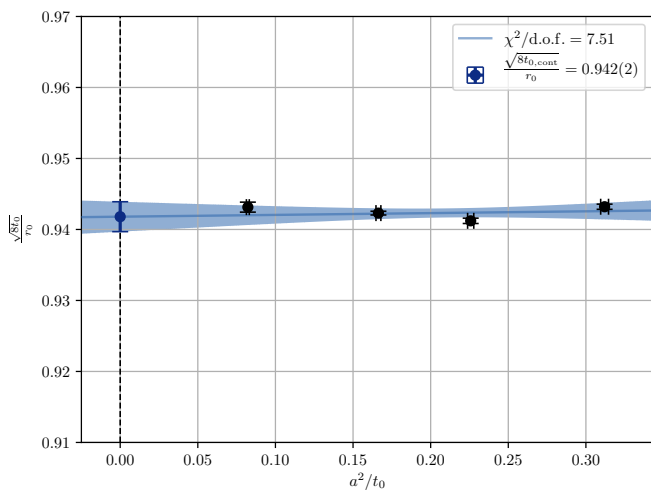


24

- We will use the clover field strength definition in gauge observables.
- Symmetries will allow us to reduce the effective number of clovers need to calculate from 24 to 6.

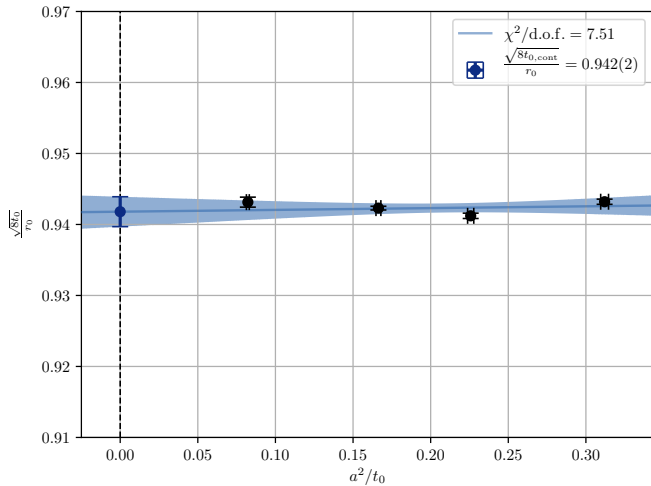


## Scale setting $t_0$



- The continuum extrapolation  $a \rightarrow 0$  for  $t_0$  of the four ensembles  $A$ ,  $B$ ,  $C$ , and  $D_2$ .

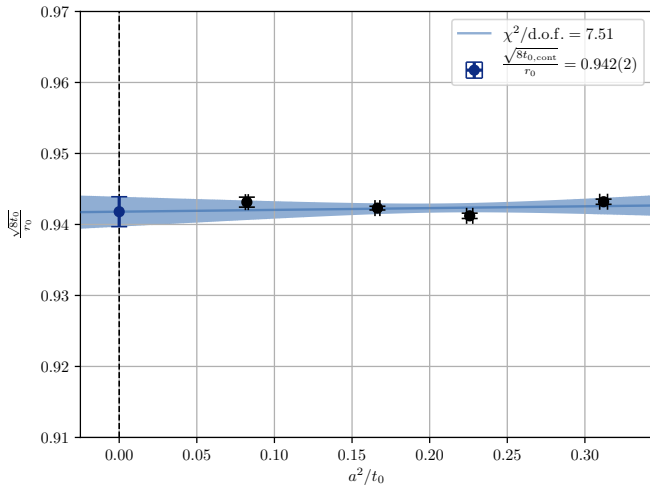
## Scale setting $t_0$



Continuum extrapolation using ensembles  $A$ ,  $B$ ,  $C$ , and  $D_2$  gives  $t_{0,\text{cont}}/r_0^2 = 0.11087(50)$ .

- The continuum extrapolation  $a \rightarrow 0$  for  $t_0$  of the four ensembles  $A$ ,  $B$ ,  $C$ , and  $D_2$ .
- $r_0 = 0.5$  fm.

## Scale setting $t_0$



Continuum extrapolation using ensembles  $A$ ,  $B$ ,  $C$ , and  $D_2$  gives  $t_{0,\text{cont}}/r_0^2 = 0.11087(50)$ . This matches the values retrieved by Lüscher [3].

26

- The continuum extrapolation  $a \rightarrow 0$  for  $t_0$  of the four ensembles  $A$ ,  $B$ ,  $C$ , and  $D_2$ .
- $r_0 = 0.5$  fm.

## Scale setting $t_0$

Extrapolations for different ensemble-combinations

Ensembles	$t_{0,\text{cont}}/r_0^2$	$\chi^2/\text{d.o.f}$
$A, B, C, D_2$	0.11087(50)	7.51
$B, C, D_2$	0.1115(3)	0.41
$A, B, C, D_1$	0.1119(6)	0.88

- Notice the  $\chi^2/\text{d.o.f.}$  of the extrapolation versus the two other extrapolations.

## Scale setting $w_0$

Can also set a scale using the derivative which offers more granularity for small flow times,

$$W(t)|_{t=w_0^2} = 0.3,$$
$$W(t) \equiv t_f \frac{d}{dt_f} \{ t_f^2 \langle E \rangle \}.$$

First presented by Borsanyi et al. [1].

## Scale setting $w_0$

Ensembles	$w_{0,\text{cont}}[\text{fm}]$	$\chi^2/\text{d.o.f}$
$A, B, C, D_2$	0.1695(5)	7.12
$B, C, D_2$	0.1702(3)	0.53
$A, B, C, D_1$	0.1706(6)	0.86

## Scale setting $w_0$

Ensembles	$w_{0,\text{cont}}[\text{fm}]$	$\chi^2/\text{d.o.f}$
$A, B, C, D_2$	0.1695(5)	7.12
$B, C, D_2$	0.1702(3)	0.53
$A, B, C, D_1$	0.1706(6)	0.86

Comparable to Borsanyi et al. [1] which included dynamical fermions, with  $w_{0,\text{cont}} = 0.1755(18)(04)$  fm.

## Topological charge

- Gauge fields can be classified by their topological properties.

## Topological charge

- Gauge fields can be classified by their topological properties.
- **Topological charge**  $Q$  can be viewed as a “measure” of instantons.

29

- Measuring **topological charge** is a measure of the *Winding number* of the gauge field.

## Topological charge

- Gauge fields can be classified by their topological properties.
- **Topological charge**  $Q$  can be viewed as a “measure” of instantons.
- **Instantons** are local minimums of the Yang-Mills action in Euclidean space.

29

- Measuring **topological charge** is a measure of the *Winding number* of the gauge field.
- **Instantons** are local minimums to the Yang-Mills action in Euclidean space.
- Instantons are significant in LQCD because of *critical slowdown* which we will return to later.

# Topological charge

- Gauge fields can be classified by their topological properties.
- **Topological charge**  $Q$  can be viewed as a “measure” of instantons.
- **Instantons** are local minimums of the Yang-Mills action in Euclidean space.

$$Q = a^4 \sum_{n \in \Lambda} q(n),$$

with the charge density given by

$$q(n) = \frac{1}{32\pi^2} \epsilon_{\mu\nu\rho\sigma} \text{tr} [F_{\mu\nu}(n) F_{\rho\sigma}(n)].$$

29

- Measuring **topological charge** is a measure of the *Winding number* of the gauge field.
- **Instantons** are local minimums to the Yang-Mills action in Euclidean space.
- Instantons are significant in LQCD because of *critical slowdown* which we will return to later.
- The charge is a **sum over the local charge** at every point in the gauge field.
- Can in a very crude manner be viewed as the “curl” of the gauge fields.

# Topological charge

- Gauge fields can be classified by their topological properties.
- **Topological charge**  $Q$  can be viewed as a “measure” of instantons.
- **Instantons** are local minimums of the Yang-Mills action in Euclidean space.

$$Q = a^4 \sum_{n \in \Lambda} q(n),$$

with the charge density given by

$$q(n) = \frac{1}{32\pi^2} \epsilon_{\mu\nu\rho\sigma} \text{tr} [F_{\mu\nu}(n) F_{\rho\sigma}(n)].$$

$$\langle Q \rangle = 0$$

29

- Measuring **topological charge** is a measure of the *Winding number* of the gauge field.
- **Instantons** are local minimums to the Yang-Mills action in Euclidean space.
- Instantons are significant in LQCD because of *critical slowdown* which we will return to later.
- The charge is a **sum over the local charge** at every point in the gauge field.
- Can in a very crude manner be viewed as the “curl” of the gauge fields.
- The **expectation value of  $Q$  is zero** due to it being **parity odd**.

# Topological charge

- Gauge fields can be classified by their topological properties.
- **Topological charge**  $Q$  can be viewed as a “measure” of instantons.
- **Instantons** are local minimums of the Yang-Mills action in Euclidean space.

$$Q = a^4 \sum_{n \in \Lambda} q(n),$$

with the charge density given by

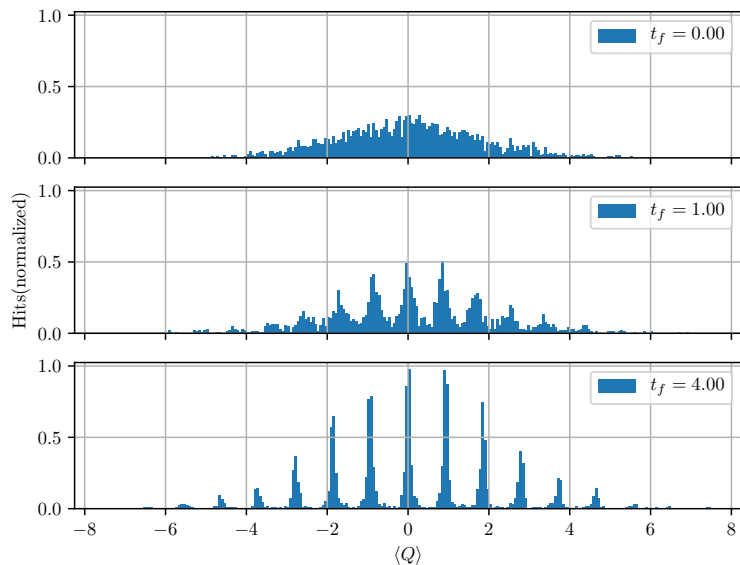
$$q(n) = \frac{1}{32\pi^2} \epsilon_{\mu\nu\rho\sigma} \text{tr} [F_{\mu\nu}(n) F_{\rho\sigma}(n)].$$

$$\langle Q \rangle = 0$$

29

- Measuring **topological charge** is a measure of the *Winding number* of the gauge field.
- **Instantons** are local minimums to the Yang-Mills action in Euclidean space.
- Instantons are significant in LQCD because of *critical slowdown* which we will return to later.
- The charge is a **sum over the local charge** at every point in the gauge field.
- Can in a very crude manner be viewed as the “curl” of the gauge fields.
- The **expectation value of  $Q$  is zero** due to it being **parity odd**.

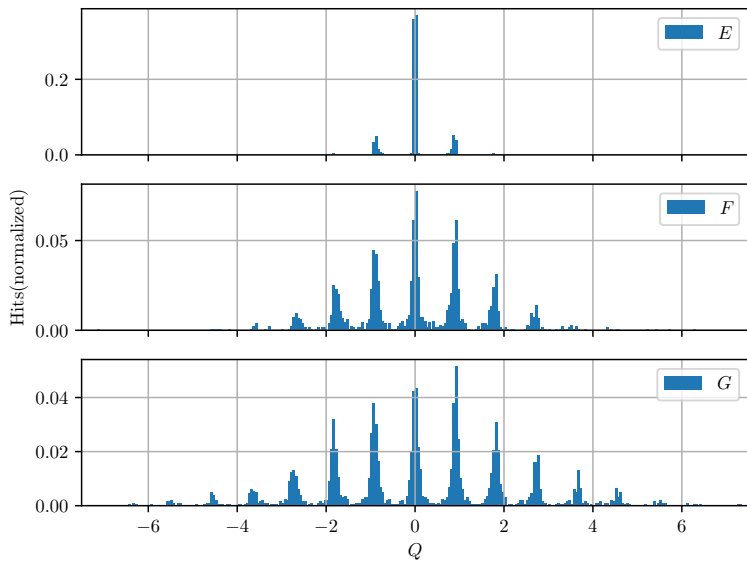
# Topological charge distribution



30

Histograms for the  $Q$  for ensemble  $G$  with a lattice of size  $N^3 \times N_T = 16^3 \times 32$  with  $\beta = 6.1$ , taken at different flow times  $t_f/a^2 = 0.0, 1.0, 4.0$  fm.

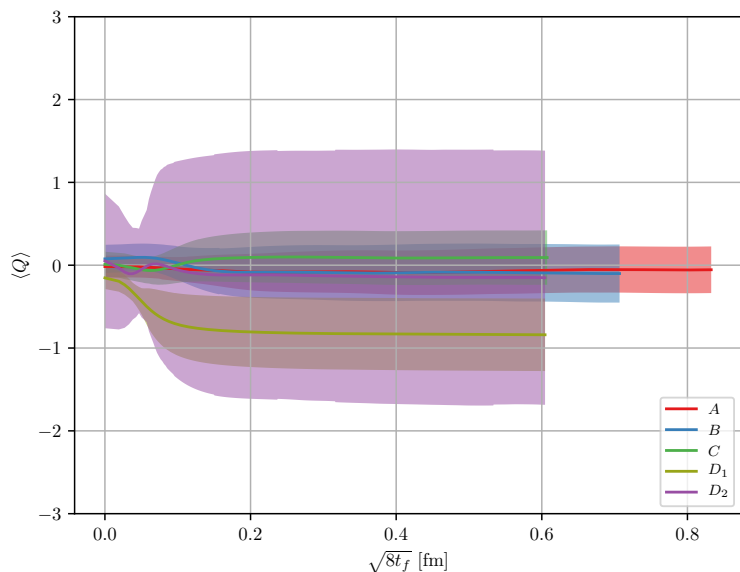
# Topological charge distribution in flow time



31

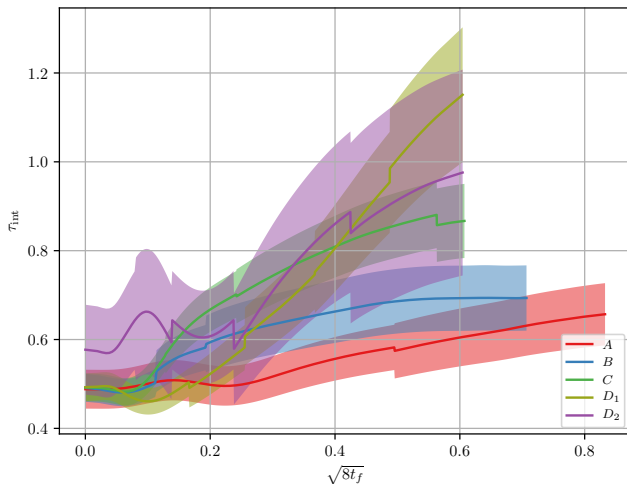
Histograms of topological charge for the supporting ensembles seen at  $t_f/a^2 = 0.25$  fm.

# Topological charge for our main ensembles



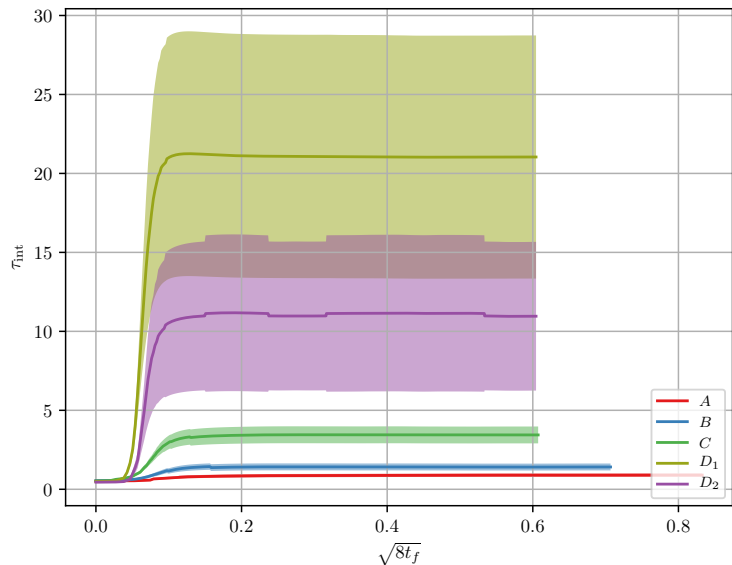
Why is the charge not centered around zero for certain ensembles?

## Autocorrelation in the energy



The autocorrelation of the energy. A value of  $\tau_{\text{int}} = 0.5$  indicates that we have zero autocorrelation.

# Topological charge autocorrelation



- The integrated autocorrelation  $\tau_{\text{int}}$  for topological charge for the five main ensembles.

## Critical slowdown

**Critical slowdown** is the phenomena where we as the lattice spacing  $a$  decreases the required energy to tunnel from one state to another increase.

## Critical slowdown

**Critical slowdown** is the phenomena where we as the lattice spacing  $a$  decreases the required energy to tunnel from one state to another *increase*.

→ many more lattice updates are required in order to have independent gauge configurations.

- That is, going from one instanton sector to another requires many more updates and becomes an inherent problem in all LQCD calculations.

## Critical slowdown

**Critical slowdown** is the phenomena where we as the lattice spacing  $a$  decreases the required energy to tunnel from one state to another *increase*.

→ many more lattice updates are required in order to have independent gauge configurations.

- That is, going from one instanton sector to another requires many more updates and becomes an inherent problem in all LQCD calculations.
- In the continuum it would require an **infinite amount of energy** to go from **one instanton sector to another**. Thus as we  $a$  approaches the **continuum**, the amount of **effort**(number of updates ect.) required to generate **independent** gauge configurations **increases**.

## Critical slowdown

**Critical slowdown** is the phenomena where we as the lattice spacing  $a$  decreases the required energy to tunnel from one state to another *increase*.

→ many more lattice updates are required in order to have independent gauge configurations.

- That is, going from one instanton sector to another requires many more updates and becomes an inherent problem in all LQCD calculations.
- In the continuum it would require an **infinite amount of energy** to go from **one instanton sector to another**. Thus as we  $a$  approaches the **continuum**, the amount of **effort**(number of updates ect.) required to generate **independent** gauge configurations **increases**.

## Topological susceptibility

The topological susceptibility is given by

$$\chi_{\text{top}}^{1/4} = \frac{1}{V^{1/4}} \langle Q^2 \rangle^{1/4}$$

with  $V$  being the lattice volume and  $\langle Q^2 \rangle$  is the second momenta of the charge.

## Topological susceptibility

The topological susceptibility is given by

$$\chi_{\text{top}}^{1/4} = \frac{1}{V^{1/4}} \langle Q^2 \rangle^{1/4}$$

with  $V$  being the lattice volume and  $\langle Q^2 \rangle$  is the second momenta of the charge.

The Witten-Veneziano relation is given by

$$m_{\eta'}^2 = \frac{2N_f}{f_\pi^2} \chi_{\text{top}}$$

- R.h.s. is full QCD and l.h.s is from pure gauge theory.

# Topological susceptibility

The topological susceptibility is given by

$$\chi_{\text{top}}^{1/4} = \frac{1}{V^{1/4}} \langle Q^2 \rangle^{1/4}$$

with  $V$  being the lattice volume and  $\langle Q^2 \rangle$  is the second momenta of the charge.

The Witten-Veneziano relation is given by

$$m_{\eta'}^2 = \frac{2N_f}{f_\pi^2} \chi_{\text{top}}$$

with

- pion decay constant  $f_\pi = 0.130(5)/\sqrt{2}$  GeV.

- R.h.s. is full QCD and l.h.s is from pure gauge theory.
- We can use the Witten-Veneziano formula in order to extract an estimate for  $N_f$  using the topological susceptibility.

# Topological susceptibility

The topological susceptibility is given by

$$\chi_{\text{top}}^{1/4} = \frac{1}{V^{1/4}} \langle Q^2 \rangle^{1/4}$$

with  $V$  being the lattice volume and  $\langle Q^2 \rangle$  is the second momenta of the charge.

The Witten-Veneziano relation is given by

$$m_{\eta'}^2 = \frac{2N_f}{f_\pi^2} \chi_{\text{top}}$$

with

- pion decay constant  $f_\pi = 0.130(5)/\sqrt{2}$  GeV.
- $\eta'$  meson mass  $m_{\eta'} = 0.95778(6)$  GeV.

- R.h.s. is full QCD and l.h.s is from pure gauge theory.
- We can use the Witten-Veneziano formula in order to extract an estimate for  $N_f$  using the topological susceptibility.

# Topological susceptibility

The topological susceptibility is given by

$$\chi_{\text{top}}^{1/4} = \frac{1}{V^{1/4}} \langle Q^2 \rangle^{1/4}$$

with  $V$  being the lattice volume and  $\langle Q^2 \rangle$  is the second momenta of the charge.

The Witten-Veneziano relation is given by

$$m_{\eta'}^2 = \frac{2N_f}{f_\pi^2} \chi_{\text{top}}$$

with

- pion decay constant  $f_\pi = 0.130(5)/\sqrt{2}$  GeV.
- $\eta'$  meson mass  $m_{\eta'} = 0.95778(6)$  GeV.
- $N_f$  is the number of flavors(i.e. quark species involved in  $\eta'$ .).

- R.h.s. is full QCD and l.h.s is from pure gauge theory.
- We can use the Witten-Veneziano formula in order to extract an estimate for  $N_f$  using the topological susceptibility.

# Topological susceptibility

The topological susceptibility is given by

$$\chi_{\text{top}}^{1/4} = \frac{1}{V^{1/4}} \langle Q^2 \rangle^{1/4}$$

with  $V$  being the lattice volume and  $\langle Q^2 \rangle$  is the second momenta of the charge.

The Witten-Veneziano relation is given by

$$m_{\eta'}^2 = \frac{2N_f}{f_\pi^2} \chi_{\text{top}}$$

with

- pion decay constant  $f_\pi = 0.130(5)/\sqrt{2}$  GeV.
- $\eta'$  meson mass  $m_{\eta'} = 0.95778(6)$  GeV.
- $N_f$  is the number of flavors(i.e. quark species involved in  $\eta'$ .).

We expect  $N_f = 3$ .

- R.h.s. is full QCD and l.h.s is from pure gauge theory.
- We can use the Witten-Veneziano formula in order to extract an estimate for  $N_f$  using the topological susceptibility.
- This can help us understand the "quality" of the ensemble, as we would expect to be around  $N_f = 3$ .

# Topological susceptibility

The topological susceptibility is given by

$$\chi_{\text{top}}^{1/4} = \frac{1}{V^{1/4}} \langle Q^2 \rangle^{1/4}$$

with  $V$  being the lattice volume and  $\langle Q^2 \rangle$  is the second momenta of the charge.

The Witten-Veneziano relation is given by

$$m_{\eta'}^2 = \frac{2N_f}{f_\pi^2} \chi_{\text{top}}$$

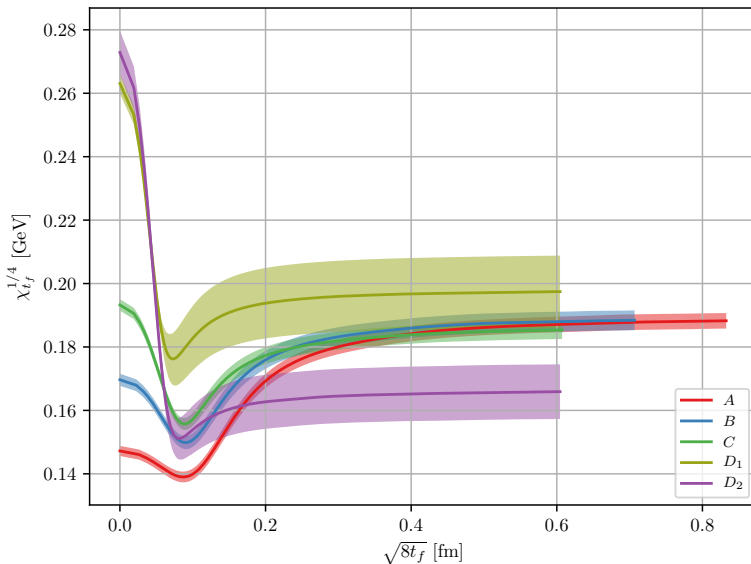
with

- pion decay constant  $f_\pi = 0.130(5)/\sqrt{2}$  GeV.
- $\eta'$  meson mass  $m_{\eta'} = 0.95778(6)$  GeV.
- $N_f$  is the number of flavors(i.e. quark species involved in  $\eta'$ .).

We expect  $N_f = 3$ .

- R.h.s. is full QCD and l.h.s is from pure gauge theory.
- We can use the Witten-Veneziano formula in order to extract an estimate for  $N_f$  using the topological susceptibility.
- This can help us understand the "quality" of the ensemble, as we would expect to be around  $N_f = 3$ .

# Topological susceptibility



38

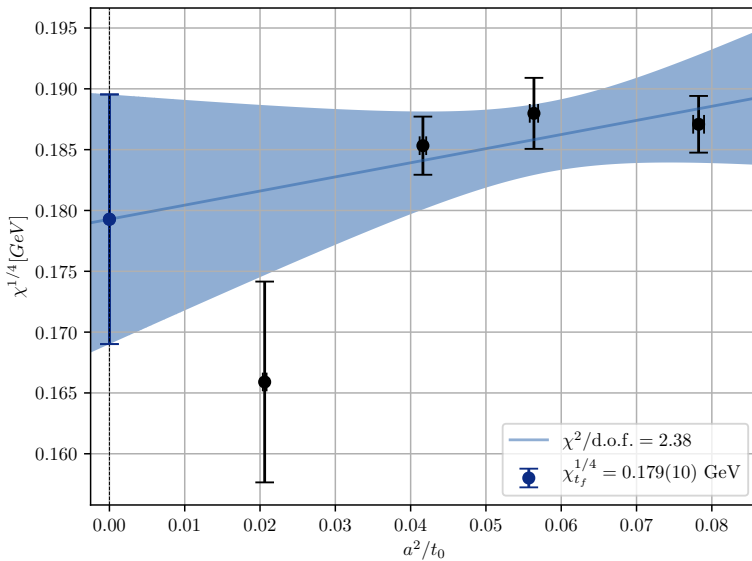
- The topological susceptibility  $\chi_{tf}^{1/4}$  of the **main ensembles**.
- We have a **UV divergence at zeroth flow time**, hence to need for gradient flow which renormalizes this quantity.
- **Bootstrapped**  $N_{\text{bs}} = 500$  times.
- **Corrected for autocorrelations** with  $\sigma = \sqrt{2\tau_{\text{int}}}\sigma_0$ .

Ensemble	$\chi_{tf}^{1/4}$ [GeV]	$\chi_{tf}^{1/4}$ [GeV], corrected	$\sqrt{2\tau_{int}}$
<i>A</i>	0.1877(23)	0.1877(24)	1.028(46)
<i>B</i>	0.1880(21)	0.1880(29)	1.346(81)
<i>C</i>	0.1853(14)	0.1853(24)	1.762(104)
<i>D</i> <sub>1</sub>	0.1971(22)	0.1971(101)	4.523(675)
<i>D</i> <sub>2</sub>	0.1656(33)	0.1656(86)	2.624(441)

Error corrected for autocorrelations with  $\sigma = \sqrt{2\tau_{int}}\sigma_0$ .

- Values extracted at a smearing radius of hadronic scales.
- The topological susceptibility for the main ensembles together with the correction factor from the integrated autocorrelation time. The second column have not had its results corrected by  $\sqrt{2\tau_{int}}$ . None of the results have been analyzed with bootstrapping.

# Topological susceptibility continuum extrapolation



- A continuum extrapolation of the topological susceptibility  $\chi_{tf}^{1/4}$  for the main ensembles excluding the  $D_1$  ensemble.
- The points for  $\chi_{tf}^{1/4}$  is taken at  $\sqrt{8t_{f,0}} = 0.6 \text{ fm}$ .

# Topological susceptibility continuum extrapolation

Ensembles	$\chi_{tf}^{1/4} (\langle Q^2 \rangle) [\text{GeV}]$	$N_f$	$\chi^2/\text{d.o.f}$
$A, B, C, D_2$	0.179(10)	3.75(29)	2.38
$A, B, C, D_1$	0.186(6)	3.21(25)	0.83
$B, C, D_1$	0.187(24)	3.18(24)	1.63
$B, C, D_2$	0.166(24)	5.06(39)	2.05
$A, B, C$	0.184(6)	3.37(26)	0.33

## The fourth cumulant

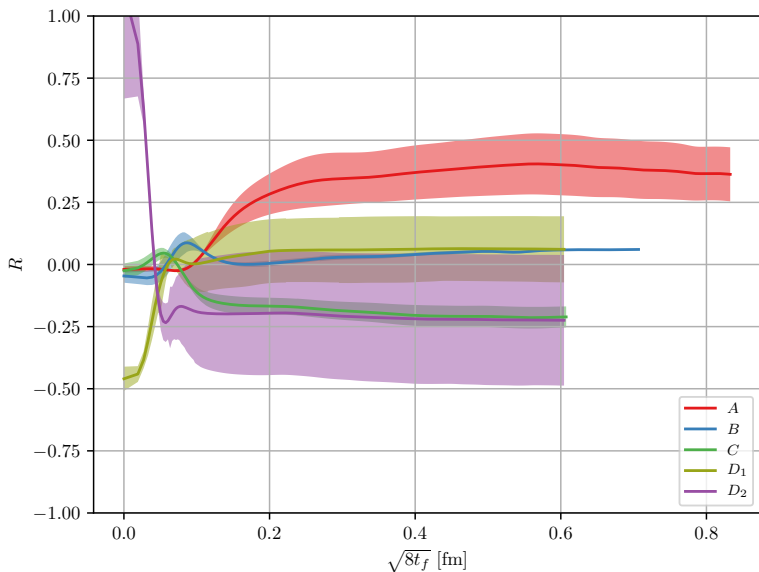
$$\langle Q^4 \rangle_c = \frac{1}{V^2} \left( \langle Q^4 \rangle - 3 \langle Q^2 \rangle^2 \right).$$

From this, we can also measure the ratio  $R$ ,

$$R = \frac{\langle Q^4 \rangle_c}{\frac{1}{V} \langle Q^2 \rangle} = \frac{1}{V} \frac{\langle Q^4 \rangle - 3 \langle Q^2 \rangle^2}{\langle Q^2 \rangle},$$

- Highly unstable, as we shall see.
- Will provide insight into the goodness of our ensembles.
- An  $R$ -value away from 1 will indicate that QCD cannot be described by the dilute instanton gas model.

## The fourth cumulant



- The fourth cumulant ratio  $R = \langle Q^4 \rangle_C / \langle Q^2 \rangle$ .
- The results was analyzed using  $N_{\text{bs}} = 500$  bootstrap samples, with the error corrected for by  $\sqrt{2\tau_{\text{int}}}$ .

# The fourth cumulant at reference flow times

Ensemble	$L/a$	$t_0/a^2$	$\langle Q^2 \rangle$	$\langle Q^4 \rangle$	$\langle Q^4 \rangle_C$	$R$
$A$	2.24	3.20(3)	0.78(4)	2.13(27)	0.282(67)	0.359(65)
$B$	2.21	4.43(4)	0.81(5)	1.98(23)	0.036(11)	0.044(11)
$C$	2.17	6.01(6)	0.77(4)	1.6(2)	-0.174(40)	-0.226(64)
$D_1$	1.53	12.2(1)	1.00(20)	3.01(1.07)	0.03(12)	0.03(12)
$D_2$	2.29	12.2(1)	0.497(100)	0.64(20)	-0.103(95)	-0.21(23)

The fourth cumulant is taken at their individual reference scales seen in the third column. The data were analyzed with using a bootstrap analysis of  $N_{bs} = 500$  samples, with error corrected by the integrated autocorrelation,  $\sqrt{2\tau_{int}}$ .

## Comparing fourth cumulant

We can compare with article by Cè et al. [2]

# Comparing fourth cumulant

Ensemble	$\beta$	$L/a$	$L$ [fm]	$a$ [fm]	$t_0/a^2$	$t_0/r_0^2$	$N_{\text{cfg}}$
$F_1$	5.96	16	1.632	0.102	2.7887(2)	0.1113(9)	1 440 000
$B_2$	6.05	14	1.218	0.087	3.7960(12)	0.1114(9)	144 000
$\tilde{D}_2$		17	1.479		3.7825(8)	0.1110(9)	
$B_3$	6.13	16	1.232	0.077	4.8855(15)	0.1113(10)	144 000
$\tilde{D}_3$		19	1.463		4.8722(11)	0.1110(10)	
$B_4$	6.21	18	1.224	0.068	6.2191(20)	0.1115(11)	144 000
$\tilde{D}_4$		21	1.428		6.1957(14)	0.1111(11)	

- Parameters of the ensembles presented by Cè et al. [2]. The first column is the ensemble name from the article. The letter indicates the volume, while the subindex indicates the  $\beta$  value. Ensembles of similar letters keep approximately the same length  $L$ .

# Comparing fourth cumulant

Ensemble	$\langle Q^2 \rangle_{\text{normed}}$	$\langle Q^4 \rangle_{\text{normed}}$	$\langle Q^4 \rangle_{C,\text{normed}}$	$R_{\text{normed}}$
$F_1$	0.728(1)	1.608(4)	0.016(1)	0.022(1)
$B_2$	0.772(3)	1.873(19)	0.085(4)	0.110(5)
$\tilde{D}_2$	0.770(3)	1.817(17)	0.037(4)	0.048(5)
$B_3$	0.760(3)	1.805(17)	0.074(3)	0.097(4)
$\tilde{D}_3$	0.769(3)	1.801(14)	0.027(1)	0.035(1)
$B_4$	0.776(3)	1.874(18)	0.069(3)	0.089(4)
$\tilde{D}_4$	0.785(3)	1.891(17)	0.040(4)	0.052(5)

- Results as presented by Cè et al. [2], **normalized by the lattice volume**.

# Comparing fourth cumulant

Article	Thesis	Ratio( $\langle Q^2 \rangle$ )	Ratio( $\langle Q^4 \rangle$ )	Ratio( $\langle Q^4 \rangle_C$ )	Ratio( $R$ )
$F_1$	$A$	1.08(6)	1.34(18)	19.03(5.81)	17.64(4.48)
$B_2$	$A$	1.02(5)	1.15(15)	3.60(1.09)	3.54(90)
	$B$	1.04(6)	1.06(11)	0.480(74)	0.46(4)
$\tilde{D}_2$	$A$	1.02(5)	1.19(15)	8.31(1.99)	8.15(1.56)
	$B$	1.05(6)	1.10(12)	1.1(1)	1.06(3)
$B_3$	$B$	1.06(6)	1.10(12)	0.550(86)	0.52(5)
$\tilde{D}_3$	$B$	1.05(6)	1.11(12)	1.51(23)	1.4(1)
$B_4$	$C$	0.99(5)	0.86(8)	-2.32(46)	-2.35(59)
$\tilde{D}_4$	$C$	0.98(5)	0.85(8)	-3.95(96)	-4.05(1.19)

- A comparison between the results obtained in this thesis on the fourth cumulant, and by those similar in volume form Cè et al. [2]. *Ratio* indicates that we are dividing our results by the ones in previous table.

# Comparing fourth cumulant

Article	Thesis	Ratio( $\langle Q^2 \rangle$ )	Ratio( $\langle Q^4 \rangle$ )	Ratio( $\langle Q^4 \rangle_C$ )	Ratio( $R$ )
$F_1$	$A$	1.08(6)	1.34(18)	19.03(5.81)	17.64(4.48)
$B_2$	$A$	1.02(5)	1.15(15)	3.60(1.09)	3.54(90)
	$B$	1.04(6)	1.06(11)	0.480(74)	0.46(4)
$\tilde{D}_2$	$A$	1.02(5)	1.19(15)	8.31(1.99)	8.15(1.56)
	$B$	1.05(6)	1.10(12)	1.1(1)	1.06(3)
$B_3$	$B$	1.06(6)	1.10(12)	0.550(86)	0.52(5)
$\tilde{D}_3$	$B$	1.05(6)	1.11(12)	1.51(23)	1.4(1)
$B_4$	$C$	0.99(5)	0.86(8)	-2.32(46)	-2.35(59)
$\tilde{D}_4$	$C$	0.98(5)	0.85(8)	-3.95(96)	-4.05(1.19)

- A comparison between the results obtained in this thesis on the fourth cumulant, and by those similar in volume form Cè et al. [2]. *Ratio* indicates that we are dividing our results by the ones in previous table.

# The topological charge correlator

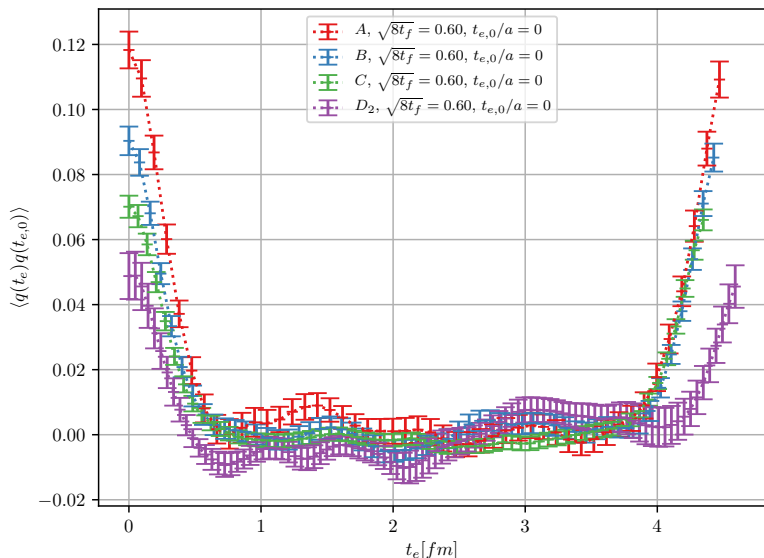
## The topological charge correlator

$$C(n_t) = \langle q(n_t)q(0) \rangle,$$

$q(0)$  is the source placed at a fixed Euclidean time, and  $q(n_t)$  is the sink which is summed across all Euclidean times.

- $q(0)$  is not required to be at  $n_t = 0$ .

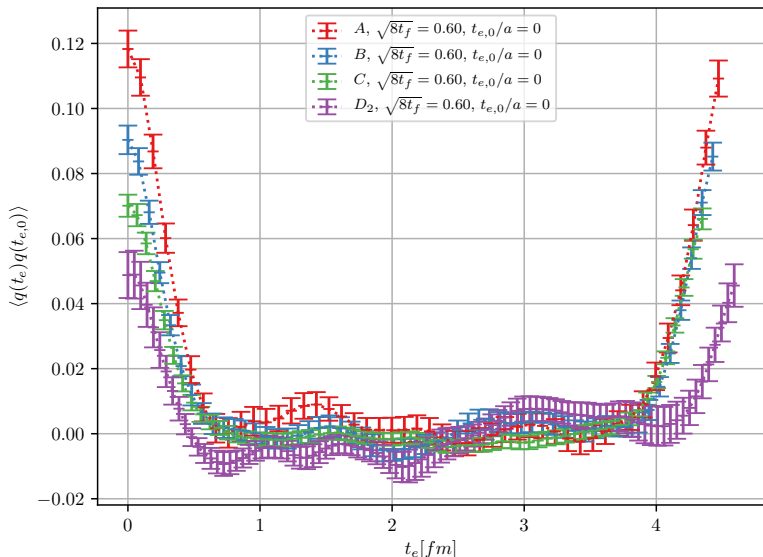
# The topological charge correlator



47

- The topological charge correlator for all of the ensembles except  $D_1$ . The  $x$ -axis contains the sink-source separation, as the source  $q(0)$  is placed at  $t_e = 0$  fm, and the sink  $q(t_e)$  is taken at  $t_e$ .

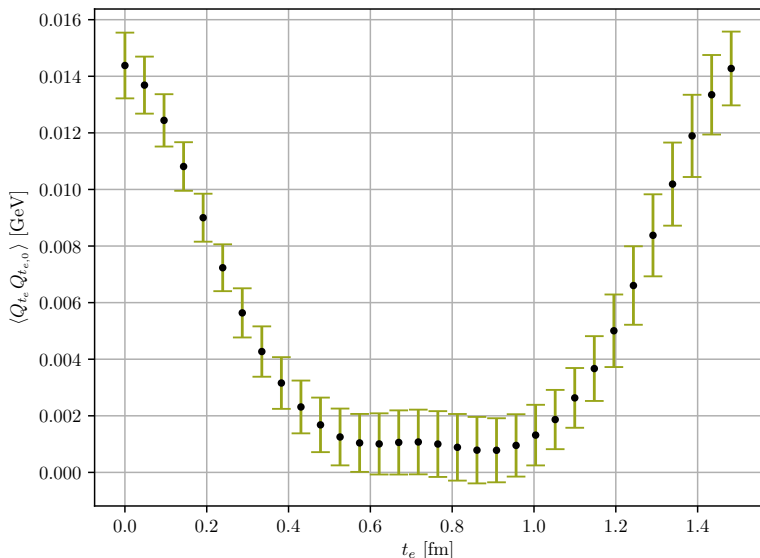
# The topological charge correlator



47

- The topological charge correlator for all of the ensembles except  $D_1$ . The  $x$ -axis contains the sink-source separation, as the source  $q(0)$  is placed at  $t_e = 0$  fm, and the sink  $q(t_e)$  is taken at  $t_e$ .
- We since the ensembles are of different lattice sizes, we plot th  $D_1$  separately.

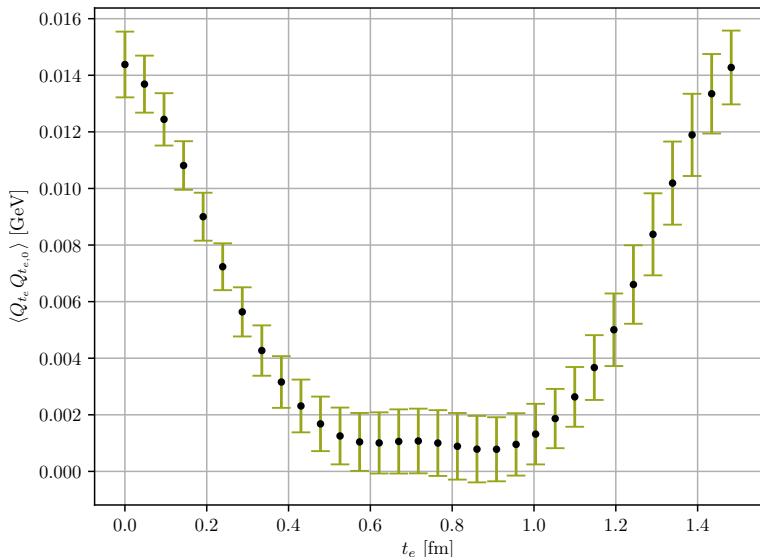
# The topological charge correlator



47

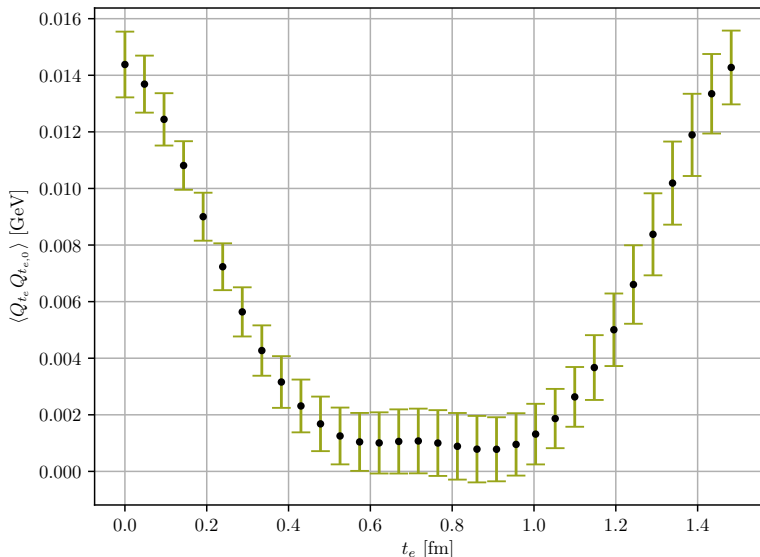
- The topological charge correlator for all of the ensembles except  $D_1$ . The  $x$ -axis contains the sink-source separation, as the source  $q(0)$  is placed at  $t_e = 0$  fm, and the sink  $q(t_e)$  is taken at  $t_e$ .
- We since the ensembles are of different lattice sizes, we plot th  $D_1$  separately.
- The topological charge correlator for the  $D_1$ . The source  $q(0)$  is placed at  $t_e = 0$  fm and the sink  $q(t_e)$  is taken at  $t_e$ .

# The topological charge correlator



- The topological charge correlator for all of the ensembles except  $D_1$ . The  $x$ -axis contains the sink-source separation, as the source  $q(0)$  is placed at  $t_e = 0$  fm, and the sink  $q(t_e)$  is taken at  $t_e$ .
- We since the ensembles are of different lattice sizes, we plot th  $D_1$  separately.
- The topological charge correlator for the  $D_1$ . The source  $q(0)$  is placed at  $t_e = 0$  fm and the sink  $q(t_e)$  is taken at  $t_e$ .
- We would expect an **exponential dampening**.

# The topological charge correlator



- The topological charge correlator for all of the ensembles except  $D_1$ . The  $x$ -axis contains the sink-source separation, as the source  $q(0)$  is placed at  $t_e = 0$  fm, and the sink  $q(t_e)$  is taken at  $t_e$ .
- We since the ensembles are of different lattice sizes, we plot th  $D_1$  separately.
- The topological charge correlator for the  $D_1$ . The source  $q(0)$  is placed at  $t_e = 0$  fm and the sink  $q(t_e)$  is taken at  $t_e$ .
- We would expect an **exponential dampening**.

## The effective glueball mass

A glueball is a bound state of gluons.

In pure Yang-Mills gauge theory, the states are stable.

We will be looking at the state involving topological charge.

## The effective glueball mass

A glueball is a bound state of gluons.

The ground state in the correlator is given as

$$C(n_t) = A_0 e^{-n_t E_0} + A_1 e^{-n_t E_1} + \dots$$

In pure Yang-Mills gauge theory, the states are stable.

We will be looking at the state involving topological charge.

## The effective glueball mass

A glueball is a bound state of gluons.

The ground state in the correlator is given as

$$C(n_t) = A_0 e^{-n_t E_0} + A_1 e^{-n_t E_1} + \dots$$

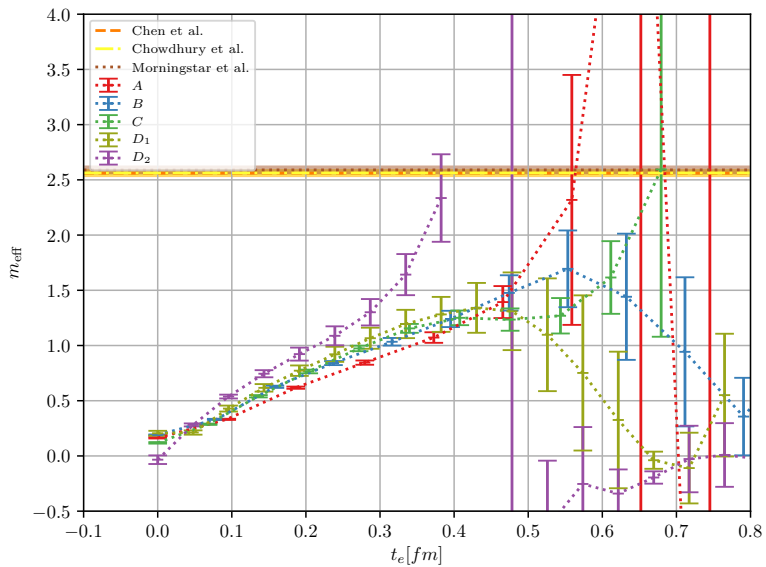
which can be extracted as

$$am_{\text{eff}} = \log \left( \frac{C(n_t)}{C(n_t + 1)} \right),$$

In pure Yang-Mills gauge theory, the states are stable.

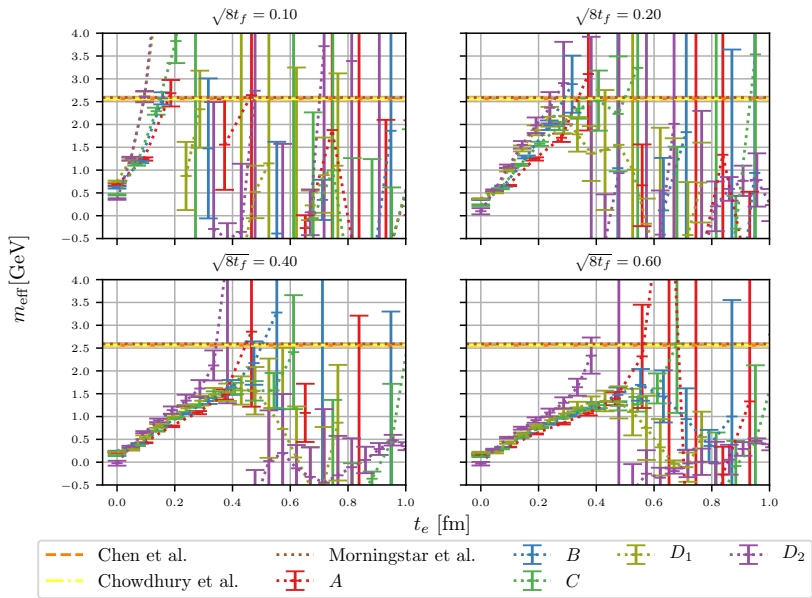
We will be looking at the state involving topological charge.

# The effective glueball mass



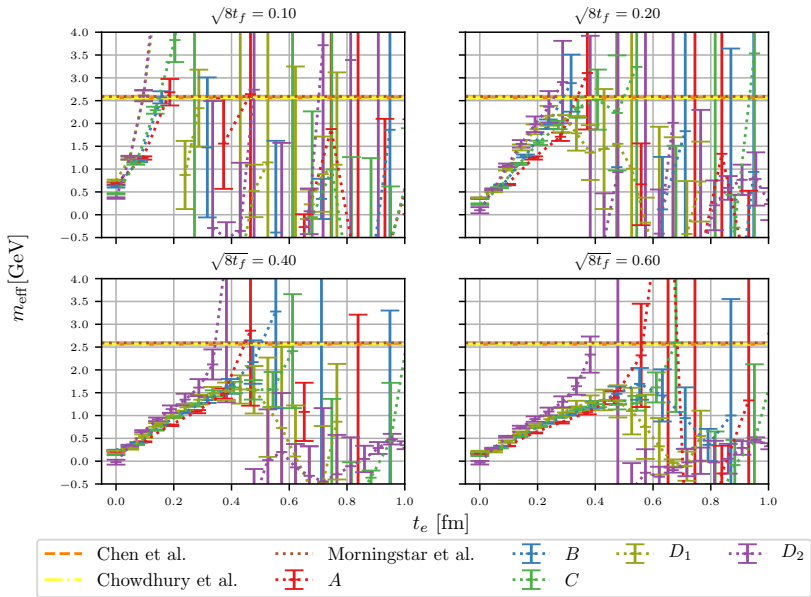
- The effective mass of the glueball, as extracted from the topological charge correlator in Euclidean time.

# The effective glueball mass



- The effective mass of the glueball, as extracted from the topological charge correlator in Euclidean time.
- Low statistics and critical slowdown → poor signal.

# The effective glueball mass



- The effective mass of the glueball, as extracted from the topological charge correlator in Euclidean time.
- Low statistics and critical slowdown → poor signal.

## Conclusion, future developments and final thoughts

---

# Conclusion

- Scaling and parameter optimizations

50

- Checked scaling and parameter optimization.

# Conclusion

- Scaling and parameter optimizations
  - Room for increased processors.

50

- Checked scaling and parameter optimization.
- We checked **strong**, **weak** and **speedup**, where we appeared to have a plateauing around 512 processors but with room for optimization.

# Conclusion

- Scaling and parameter optimizations
  - Room for increased processors.
  - $N_{\text{up}} > N_{\text{corr}}$

50

- Checked scaling and parameter optimization.
- We checked **strong**, **weak** and **speedup**, where we appeared to have a plateauing around 512 processors but with room for optimization.
- $N_{\text{up}}$  could be increased, as it has a smaller impact than  $N_{\text{corr}}$ .

# Conclusion

- Scaling and parameter optimizations
  - Room for increased processors.
  - $N_{\text{up}} > N_{\text{corr}}$
  - Machine precision accuracy when comparing with Chroma.

50

- Checked scaling and parameter optimization.
- We checked **strong**, **weak** and **speedup**, where we appeared to have a plateauing around 512 processors but with room for optimization.
- $N_{\text{up}}$  could be increased, as it has a smaller impact than  $N_{\text{corr}}$ .
- Same results as Chroma down to machine precision.
- We also checked the  $\epsilon_{\text{rnd}}$  for matrix generation parameter that it minimized the autocorrelation, and the integration step  $\epsilon_f$ .

# Conclusion

- Scaling and parameter optimizations
  - Room for increased processors.
  - $N_{\text{up}} > N_{\text{corr}}$
  - Machine precision accuracy when comparing with Chroma.
- $t_0$  and  $w_0$  match other papers, e.g. Lüscher [3] and Cè et al. [2].

50

- Checked scaling and parameter optimization.
- We checked **strong**, **weak** and **speedup**, where we appeared to have a plateauing around 512 processors but with room for optimization.
- $N_{\text{up}}$  could be increased, as it has a smaller impact than  $N_{\text{corr}}$ .
- Same results as Chroma down to machine precision.
- We also checked the  $\epsilon_{\text{rnd}}$  for matrix generation parameter that it minimized the autocorrelation, and the integration step  $\epsilon_f$ .
- $t_0$  and  $w_0$  match other papers.

# Conclusion

- Scaling and parameter optimizations
  - Room for increased processors.
  - $N_{\text{up}} > N_{\text{corr}}$
  - Machine precision accuracy when comparing with Chroma.
- $t_0$  and  $w_0$  match other papers, e.g. Lüscher [3] and Cè et al. [2].
- $\langle Q \rangle \neq 0$  for some ensembles.

50

- Checked scaling and parameter optimization.
- We checked **strong**, **weak** and **speedup**, where we appeared to have a plateauing around 512 processors but with room for optimization.
- $N_{\text{up}}$  could be increased, as it has a smaller impact than  $N_{\text{corr}}$ .
- Same results as Chroma down to machine precision.
- We also checked the  $\epsilon_{\text{rnd}}$  for matrix generation parameter that it minimized the autocorrelation, and the integration step  $\epsilon_f$ .
- $t_0$  and  $w_0$  match other papers.
- $\langle Q \rangle$

# Conclusion

- Scaling and parameter optimizations
  - Room for increased processors.
  - $N_{\text{up}} > N_{\text{corr}}$
  - Machine precision accuracy when comparing with Chroma.
- $t_0$  and  $w_0$  match other papers, e.g. Lüscher [3] and Cè et al. [2].
- $\langle Q \rangle \neq 0$  for some ensembles.
- The topological susceptibility  $\langle \chi_f^{1/4} \rangle$  and  $N_f$

50

- Checked scaling and parameter optimization.
- We checked **strong**, **weak** and **speedup**, where we appeared to have a plateauing around 512 processors but with room for optimization.
- $N_{\text{up}}$  could be increased, as it has a smaller impact than  $N_{\text{corr}}$ .
- Same results as Chroma down to machine precision.
- We also checked the  $\epsilon_{\text{rnd}}$  for matrix generation parameter that it minimized the autocorrelation, and the integration step  $\epsilon_f$ .
- $t_0$  and  $w_0$  match other papers.
- $\langle Q \rangle$
- $\chi_f^{1/4}$ . Matches well with other papers

# Conclusion

- Scaling and parameter optimizations
  - Room for increased processors.
  - $N_{\text{up}} > N_{\text{corr}}$
  - Machine precision accuracy when comparing with Chroma.
- $t_0$  and  $w_0$  match other papers, e.g. Lüscher [3] and Cè et al. [2].
- $\langle Q \rangle \neq 0$  for some ensembles.
- The topological susceptibility  $\langle \chi_f^{1/4} \rangle$  and  $N_f$
- $\langle Q^4 \rangle_C$  and  $R$ . Sensitive quantities - need large statistics.

50

- Checked scaling and parameter optimization.
- We checked **strong**, **weak** and **speedup**, where we appeared to have a plateauing around 512 processors but with room for optimization.
- $N_{\text{up}}$  could be increased, as it has a smaller impact than  $N_{\text{corr}}$ .
- Same results as Chroma down to machine precision.
- We also checked the  $\epsilon_{\text{rnd}}$  for matrix generation parameter that it minimized the autocorrelation, and the integration step  $\epsilon_f$ .
- $t_0$  and  $w_0$  match other papers.
- $\langle Q \rangle$
- $\chi_f^{1/4}$ . Matches well with other papers
- $\langle Q^4 \rangle_C$  and  $R$ . Sensitive quantity, matches well of first and second moment.

# Conclusion

- Scaling and parameter optimizations
  - Room for increased processors.
  - $N_{\text{up}} > N_{\text{corr}}$
  - Machine precision accuracy when comparing with Chroma.
- $t_0$  and  $w_0$  match other papers, e.g. Lüscher [3] and Cè et al. [2].
- $\langle Q \rangle \neq 0$  for some ensembles.
- The topological susceptibility  $\langle \chi_f^{1/4} \rangle$  and  $N_f$
- $\langle Q^4 \rangle_C$  and  $R$ . Sensitive quantities - need large statistics.
- Topological charge correlator  $\langle q(n_t)q(0) \rangle$  and glueball mass.

50

- Checked scaling and parameter optimization.
- We checked **strong**, **weak** and **speedup**, where we appeared to have a plateauing around 512 processors but with room for optimization.
- $N_{\text{up}}$  could be increased, as it has a smaller impact than  $N_{\text{corr}}$ .
- Same results as Chroma down to machine precision.
- We also checked the  $\epsilon_{\text{rnd}}$  for matrix generation parameter that it minimized the autocorrelation, and the integration step  $\epsilon_f$ .
- $t_0$  and  $w_0$  match other papers.
- $\langle Q \rangle$
- $\chi_f^{1/4}$ . Matches well with other papers
- $\langle Q^4 \rangle_C$  and  $R$ . Sensitive quantity, matches well of first and second moment.
- Topological charge correlator  $\langle q(n_t)q(0) \rangle$  and glueball mass.

# Conclusion

- Scaling and parameter optimizations
  - Room for increased processors.
  - $N_{\text{up}} > N_{\text{corr}}$
  - Machine precision accuracy when comparing with Chroma.
- $t_0$  and  $w_0$  match other papers, e.g. Lüscher [3] and Cè et al. [2].
- $\langle Q \rangle \neq 0$  for some ensembles.
- The topological susceptibility  $\langle \chi_f^{1/4} \rangle$  and  $N_f$
- $\langle Q^4 \rangle_C$  and  $R$ . Sensitive quantities - need large statistics.
- Topological charge correlator  $\langle q(n_t)q(0) \rangle$  and glueball mass.
- Statistics, autocorrelation and critical slowdown.

50

- Checked scaling and parameter optimization.
- We checked **strong**, **weak** and **speedup**, where we appeared to have a plateauing around 512 processors but with room for optimization.
- $N_{\text{up}}$  could be increased, as it has a smaller impact than  $N_{\text{corr}}$ .
- Same results as Chroma down to machine precision.
- We also checked the  $\epsilon_{\text{rnd}}$  for matrix generation parameter that it minimized the autocorrelation, and the integration step  $\epsilon_f$ .
- $t_0$  and  $w_0$  match other papers.
- $\langle Q \rangle$
- $\chi_f^{1/4}$ . Matches well with other papers
- $\langle Q^4 \rangle_C$  and  $R$ . Sensitive quantity, matches well of first and second moment.
- Topological charge correlator  $\langle q(n_t)q(0) \rangle$  and glueball mass.
- Critical slowdown, which makes transitioning to a new, independent configuration difficult. This inhibits the gathering of statistics, and helps us explain why we for larger  $\beta$  values have fewer independent gauge configurations.

# Conclusion

- Scaling and parameter optimizations
  - Room for increased processors.
  - $N_{\text{up}} > N_{\text{corr}}$
  - Machine precision accuracy when comparing with Chroma.
- $t_0$  and  $w_0$  match other papers, e.g. Lüscher [3] and Cè et al. [2].
- $\langle Q \rangle \neq 0$  for some ensembles.
- The topological susceptibility  $\langle \chi_f^{1/4} \rangle$  and  $N_f$
- $\langle Q^4 \rangle_C$  and  $R$ . Sensitive quantities - need large statistics.
- Topological charge correlator  $\langle q(n_t)q(0) \rangle$  and glueball mass.
- Statistics, autocorrelation and critical slowdown.

50

- Checked scaling and parameter optimization.
- We checked **strong**, **weak** and **speedup**, where we appeared to have a plateauing around 512 processors but with room for optimization.
- $N_{\text{up}}$  could be increased, as it has a smaller impact than  $N_{\text{corr}}$ .
- Same results as Chroma down to machine precision.
- We also checked the  $\epsilon_{\text{rnd}}$  for matrix generation parameter that it minimized the autocorrelation, and the integration step  $\epsilon_f$ .
- $t_0$  and  $w_0$  match other papers.
- $\langle Q \rangle$
- $\chi_f^{1/4}$ . Matches well with other papers
- $\langle Q^4 \rangle_C$  and  $R$ . Sensitive quantity, matches well of first and second moment.
- Topological charge correlator  $\langle q(n_t)q(0) \rangle$  and glueball mass.
- Critical slowdown, which makes transitioning to a new, independent configuration difficult. This inhibits the gathering of statistics, and helps us explain why we for larger  $\beta$  values have fewer independent gauge configurations.

## Future developments and final thoughts

- Better statistics.

## Future developments and final thoughts

- Better statistics.
- Better utilization of support ensembles  $E$ ,  $F$  and  $G$ .

## Future developments and final thoughts

- Better statistics.
- Better utilization of support ensembles  $E$ ,  $F$  and  $G$ .
- Improve autocorrelation with larger  $N_{\text{up}}$ .

## Future developments and final thoughts

- Better statistics.
- Better utilization of support ensembles  $E$ ,  $F$  and  $G$ .
- Improve autocorrelation with larger  $N_{\text{up}}$ .
- Implement better actions with and operators containing errors.

## Future developments and final thoughts

- Better statistics.
- Better utilization of support ensembles  $E$ ,  $F$  and  $G$ .
- Improve autocorrelation with larger  $N_{\text{up}}$ .
- Implement better actions with and operators containing errors.
- Fermions and HMC(Hybrid Monte Carlo).

Questions?

## References

---

- [1] S. Borsanyi, S. Durr, Z. Fodor, C. Hoelbling, S. D. Katz, S. Krieg, T. Kurth, L. Lellouch, T. Lippert, C. McNeile, and K. K. Szabo. High-precision scale setting in lattice QCD. *Journal of High Energy Physics*, 2012(9), September 2012. ISSN 1029-8479. doi: 10.1007/JHEP09(2012)010. URL <http://arxiv.org/abs/1203.4469>. arXiv: 1203.4469.
- [2] Marco Cè, Cristian Consonni, Georg P. Engel, and Leonardo Giusti. Non-Gaussianities in the topological charge distribution of the SU(3) Yang-Mills theory. *Physical Review D*, 92(7), October 2015. ISSN 1550-7998, 1550-2368. doi: 10.1103/PhysRevD.92.074502. URL <http://arxiv.org/abs/1506.06052>. arXiv: 1506.06052.
- [3] Martin Lüscher. Properties and uses of the Wilson flow in lattice QCD. *Journal of High Energy Physics*, 2010(8), August 2010. ISSN 1029-8479. doi: 10.1007/JHEP08(2010)071. URL <http://arxiv.org/abs/1006.4518>. arXiv: 1006.4518.

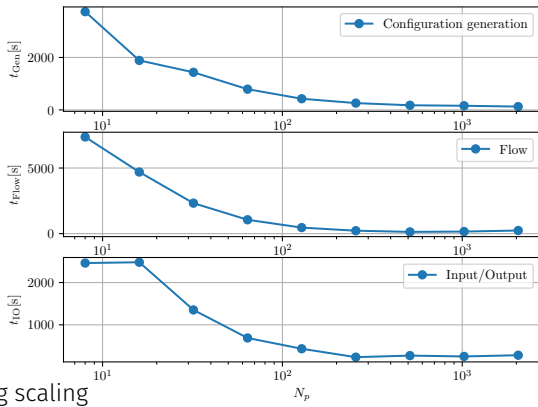
## Extras

---

# Scaling

We checked three types of scaling,

- Strong scaling: fixed problem and a variable  $N_p$  cores

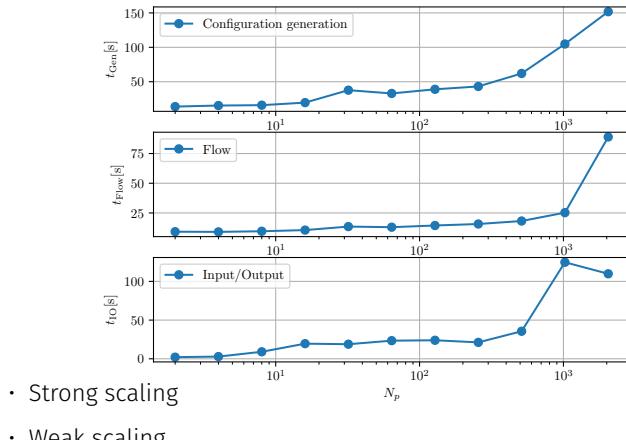


- Strong scaling

# Scaling

We checked three types of scaling,

- **Strong scaling:** *fixed problem* and a *variable  $N_p$  cores*
- **Weak scaling:** *fixed problem per processor* and a *variable  $N_p$  cores.*

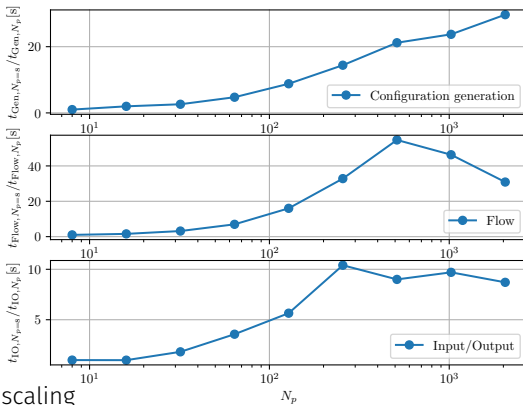


- Strong scaling
- Weak scaling

# Scaling

We checked three types of scaling,

- **Strong scaling:** *fixed problem* and a *variable  $N_p$  cores*
- **Weak scaling:** *fixed problem per processor* and a *variable  $N_p$  cores*.
- **Speedup:** defined as  $S(p) = \frac{t_{N_p}}{t_{N_p=0}}$ .



- Strong scaling
- Weak scaling
- The speedup of the configuration generation, flowing, and IO. The speedup is calculated by dividing the run time of each  $N_p$  run, with the run time of the run with the least number of processors,  $N_p = 8$ .

# Scaling

We checked three types of scaling,

- **Strong scaling:** *fixed problem and a variable  $N_p$  cores*
- **Weak scaling:** *fixed problem per processor and a variable  $N_p$  cores.*
- **Speedup:** defined as  $S(p) = \frac{t_{N_p}}{t_{N_p,0}}$ .

54

- Strong scaling
- Weak scaling
- The speedup of the configuration generation, flowing, and IO. The speedup is calculated by dividing the run time of each  $N_p$  run, with the run time of the run with the least number of processors,  $N_p = 8$ .
- The IO was optimized later to be a factor of ten or more faster.

# Scaling

We checked three types of scaling,

- **Strong scaling:** *fixed problem and a variable  $N_p$  cores*
- **Weak scaling:** *fixed problem per processor and a variable  $N_p$  cores.*
- **Speedup:** defined as  $S(p) = \frac{t_{N_p}}{t_{N_p,0}}$ .

We appear to have a plateau around 512 cores.

- Strong scaling
- Weak scaling
- The speedup of the configuration generation, flowing, and IO. The speedup is calculated by dividing the run time of each  $N_p$  run, with the run time of the run with the least number of processors,  $N_p = 8$ .
- The IO was optimized later to be a factor of ten or more faster.

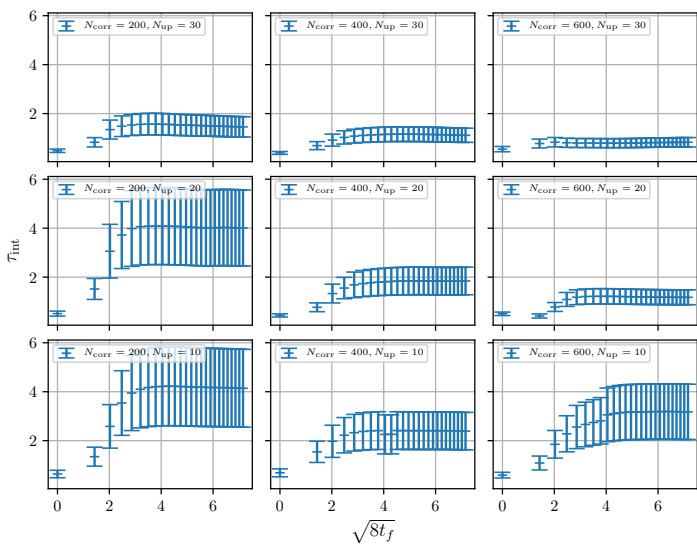
# Optimizing the gauge configuration generation

Generated 200 configurations for a lattice of size  $N^3 \times N_T = 16^3 \times 32$  and  $\beta = 6.0$ , for combinations of  $N_{\text{corr}} \in [200, 400, 600]$  and  $N_{\text{up}} \in [10, 20, 30]$ .

55

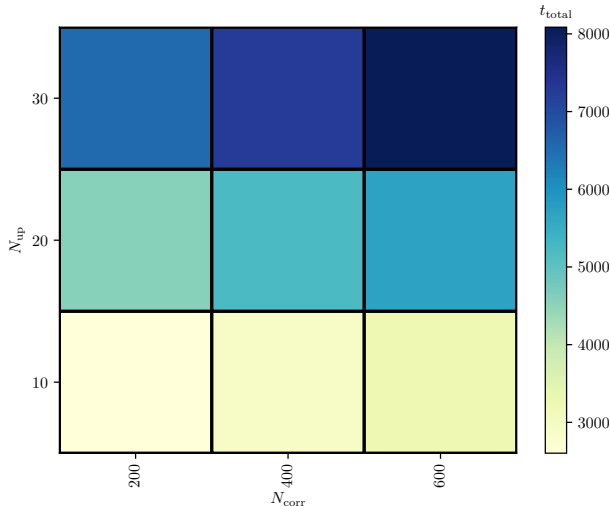
- We run for different values for  $N_{\text{up}}$  and  $N_{\text{corr}}$  to see what gives optimizes **computational cost** and **autocorrelation**.
- The integrated autocorrelation time for topological charge  $\langle Q \rangle$  for a lattice of size  $N = 16$  and  $N_T = 32$  with  $\beta = 6.0$  for combinations of  $N_{\text{corr}} \in [200, 400, 600]$  and  $N_{\text{up}} \in [10, 20, 30]$ , plotted against flow time  $\sqrt{8t_f}$ .

# Optimizing the gauge configuration generation



- We run for different values for  $N_{\text{up}}$  and  $N_{\text{corr}}$  to see what gives optimizes **computational cost** and **autocorrelation**.
- The integrated autocorrelation time for topological charge  $\langle Q \rangle$  for a lattice of size  $N = 16$  and  $N_T = 32$  with  $\beta = 6.0$  for combinations of  $N_{\text{corr}} \in [200, 400, 600]$  and  $N_{\text{up}} \in [10, 20, 30]$ , plotted against flow time  $\sqrt{8t_f}$ .
- The time taking to generate 200 configurations and flowing them  $N_{\text{flow}} = 250$  flow steps for a lattice of size  $N = 16$  and  $N_T = 32$ , with  $\beta = 6.0$  for combinations of  $N_{\text{corr}} \in [200, 400, 600]$  and  $N_{\text{up}} \in [10, 20, 30]$ .

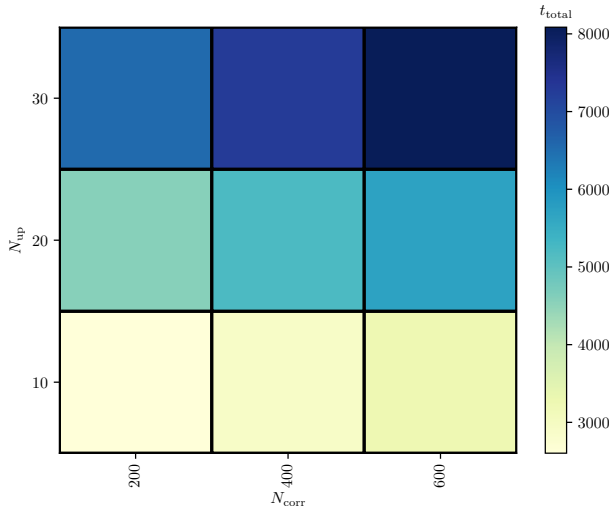
# Optimizing the gauge configuration generation



55

- We run for different values for  $N_{\text{up}}$  and  $N_{\text{corr}}$  to see what gives optimizes **computational cost** and **autocorrelation**.
- The integrated autocorrelation time for topological charge  $\langle Q \rangle$  for a lattice of size  $N = 16$  and  $N_T = 32$  with  $\beta = 6.0$  for combinations of  $N_{\text{corr}} \in [200, 400, 600]$  and  $N_{\text{up}} \in [10, 20, 30]$ , plotted against flow time  $\sqrt{8t_f}$ .
- The time taking to generate 200 configurations and flowing them  $N_{\text{flow}} = 250$  flow steps for a lattice of size  $N = 16$  and  $N_T = 32$ , with  $\beta = 6.0$  for combinations of  $N_{\text{corr}} \in [200, 400, 600]$  and  $N_{\text{up}} \in [10, 20, 30]$ .
- What we see is that increasing  $N_{\text{up}}$  is a cheaper alternative compared to using  $N_{\text{corr}}$

# Optimizing the gauge configuration generation



55

- We run for different values for  $N_{\text{up}}$  and  $N_{\text{corr}}$  to see what gives optimizes **computational cost** and **autocorrelation**.
- The integrated autocorrelation time for topological charge  $\langle Q \rangle$  for a lattice of size  $N = 16$  and  $N_T = 32$  with  $\beta = 6.0$  for combinations of  $N_{\text{corr}} \in [200, 400, 600]$  and  $N_{\text{up}} \in [10, 20, 30]$ , plotted against flow time  $\sqrt{8t_f}$ .
- The time taking to generate 200 configurations and flowing them  $N_{\text{flow}} = 250$  flow steps for a lattice of size  $N = 16$  and  $N_T = 32$ , with  $\beta = 6.0$  for combinations of  $N_{\text{corr}} \in [200, 400, 600]$  and  $N_{\text{up}} \in [10, 20, 30]$ .
- What we see is that increasing  $N_{\text{up}}$  is a cheaper alternative compared to using  $N_{\text{corr}}$

## Verifying the code

- Unit testing. SU(3), SU(2) multiplications.

## Verifying the code

- **Unit testing.** SU(3), SU(2) multiplications.
- **Integration testing.** Random matrix generation, lattice objects, parallelization, ect.

## Verifying the code

- **Unit testing.** SU(3), SU(2) multiplications.
- **Integration testing.** Random matrix generation, lattice objects, parallelization, ect.
- **Validation testing.** Cross checking results with a configuration from Chroma.

## Additional ensembles

Ensemble	$N$	$N_T$	$N_{\text{cfg}}$	$N_{\text{corr}}$	$N_{\text{up}}$	$a$ [fm]	$L$ [fm]
$E$	8	16	8135	600	30	0.0931(4)	0.745(3)
$F$	12	24	1341	200	20	0.0931(4)	1.118(5)
$G$	16	32	2000	400	20	0.0790(3)	1.265(6)

- Additional ensembles made in order to illuminate additional aspects of the topological charge.
- Supporting ensembles made on Smaug. All ensembles were flown  $N_{\text{flow}} = 1000$  steps with  $\epsilon_{\text{flow}} = 0.01$ .